

HETEROCYCLES, Vol. 106, No. 10, 2023, pp. 1649 - 1686. © 2023 The Japan Institute of Heterocyclic Chemistry
Received, 22nd May, 2023, Accepted, 22nd June, 2023, Published online, 5th July, 2023
DOI: 10.3987/REV-23-1011

ASYMMETRIC INVERSE-ELECTRON-DEMAND 1,3-DIPOLAR CYCLOADDITIONS USING ORGANOCATALYSTS

Hiroyuki Suga* and Yasunori Toda

Department of Materials Chemistry, Faculty of Engineering, Shinshu University,
Nagano 380-8553, Japan, sugahio@shinshu-u.ac.jp

Abstract – 1,3-Dipolar cycloaddition reactions have been utilized as a powerful tool for the construction of five-membered heterocyclic rings in organic synthesis because of their stereospecificity and regioselectivity. A large number of chiral Lewis acid-catalyzed asymmetric 1,3-dipolar cycloadditions for both normal- and inverse-electron-demand types have already been reported. Asymmetric normal-electron-demand 1,3-dipolar cycloadditions have also been well studied in organocatalysis, and a significant number of examples have been reported. In contrast, successful examples of asymmetric inverse-electron-demand 1,3-dipolar cycloadditions using organocatalysts are currently limited. This review focuses on chiral organic molecule-mediated enantioselective inverse-electron-demand 1,3-dipolar cycloaddition reactions. For 1,3-dipoles, we mainly cover nitrones, *C,N*-cyclic azomethine imines, *N,N*-cyclic azomethine imines, and nitrile oxides. Similar types of inverse-electron-demand [3+2] cycloadditions are described, employing hydrazones, oxaziridines, and azo compounds. Among the organocatalyst-mediated asymmetric inverse-electron-demand cycloadditions, more examples were found for using azomethine imines than for other 1,3-dipoles. *N*-Triflylphosphoramides, phosphoric acids, amines, *N*-heterocyclic carbenes, amine-thioureas, and amine-ureas, depending on which 1,3-dipoles or dipolarophiles are used, would be the chiral catalyst of choice for achieving asymmetric inverse-electron-demand 1,3-dipolar cycloadditions.

CONTENTS

1. Introduction
2. Nitron Cycloadditions
3. Azomethine Imine Cycloadditions

- 3-1. *C,N*-Cyclic Azomethine Imine Cycloaddition
- 3-2. *N,N*-Cyclic Azomethine Imine Cycloaddition
- 3-3. Hydrazones as Precursors
4. Nitrile Oxide Cycloadditions
5. Similar Types of Formal [3+2] Cycloaddition
 - 5-1. Oxaziridines as 1,3-Dipole Equivalents
 - 5-2. Azo Compounds as 1,3-Dipole Equivalents
6. Conclusion

1. INTRODUCTION

1,3-Dipolar cycloaddition reactions are among the most powerful tools for the construction of five-membered heterocyclic rings in organic synthesis.¹ The reactions have been utilized as a common method for the synthesis of optically active five-membered heterocycles involving natural products and biologically important compounds with continuous stereogenic centers due to their stereospecificity and regioselectivity.² Classically, diastereoselectivity in 1,3-dipolar cycloadditions has been studied using chiral 1,3-dipoles or chiral dipolarophiles to reveal the stereochemical outcomes that optimize the synthetic design of optically active complex molecules.³ The catalytic asymmetric version of 1,3-dipolar cycloaddition has also been extensively investigated and accounts for a large field of research.⁴ Depending on which reactants (1,3-dipoles or dipolarophiles) are activated by the catalyst, the mode of cycloaddition can be classified by the frontier molecular orbital (FMO) theory. According to the traditional Sustman classification, 1,3-dipolar cycloadditions are classified into three types as follows: type I involving a $\text{HOMO}_{\text{dipole}}\text{-LUMO}_{\text{dipolarophile}}$ interaction, type II involving both $\text{HOMO}_{\text{dipole}}\text{-LUMO}_{\text{dipolarophile}}$ and $\text{LUMO}_{\text{dipole}}\text{-HOMO}_{\text{dipolarophile}}$ interactions, and type III involving a $\text{LUMO}_{\text{dipole}}\text{-HOMO}_{\text{dipolarophile}}$ interaction based on the relative FMO energies between the 1,3-dipoles and the dipolarophiles (Figure 1).⁵ Although Sustman similarly classified Diels-Alder reactions into three types, a simple binary classification of normal-electron-demand (NED) by a $\text{HOMO}_{\text{diene}}\text{-LUMO}_{\text{dienophile}}$ interaction and inverse-electron-demand (IED) by a $\text{LUMO}_{\text{diene}}\text{-HOMO}_{\text{dienophile}}$ has been frequently used. Classification in terms of the NED and IED would be more familiar for the 1,3-dipolar cycloaddition reactions using catalysts that affect the FMO by reducing the energy difference between the HOMO and LUMO (Figure 2).⁶ We use these terms for the classification in this review. Although the reactions are classified as Sustman's type II if some 1,3-dipoles act as both the LUMO and HOMO, the LUMO of either the 1,3-dipoles or dipolarophiles could be activated by Lewis acids. Probably due to the simplicity of the reaction design, at the present time, a large number of chiral Lewis acid-catalyzed asymmetric reactions have already been reported for both NED and IED 1,3-dipolar cycloadditions. Because LUMO activation of dienophiles by organocatalysts has also become a general

technique in asymmetric Diels-Alder reactions, there are many examples of organocatalyzed-asymmetric NED 1,3-dipolar cycloadditions. These reports have been well-covered in several previous reviews.⁴ In contrast, successful examples of asymmetric IED 1,3-dipolar cycloadditions using organocatalysts are limited. In this review, we focus mainly on the asymmetric IED 1,3-dipolar cycloadditions by organocatalysis.

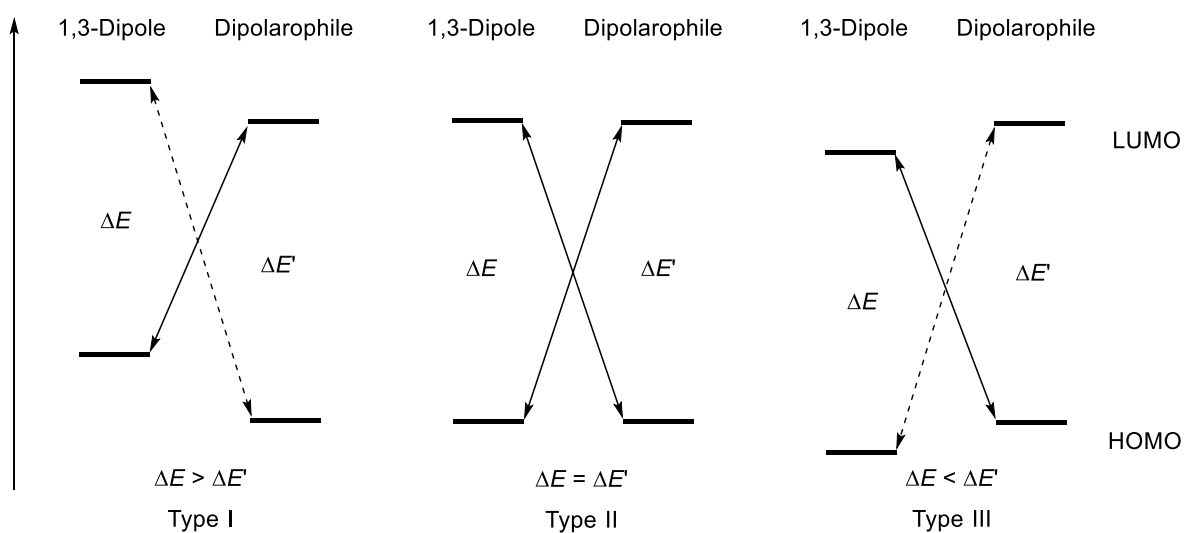


Figure 1. Sustman classification of 1,3-dipolar cycloaddition reactions

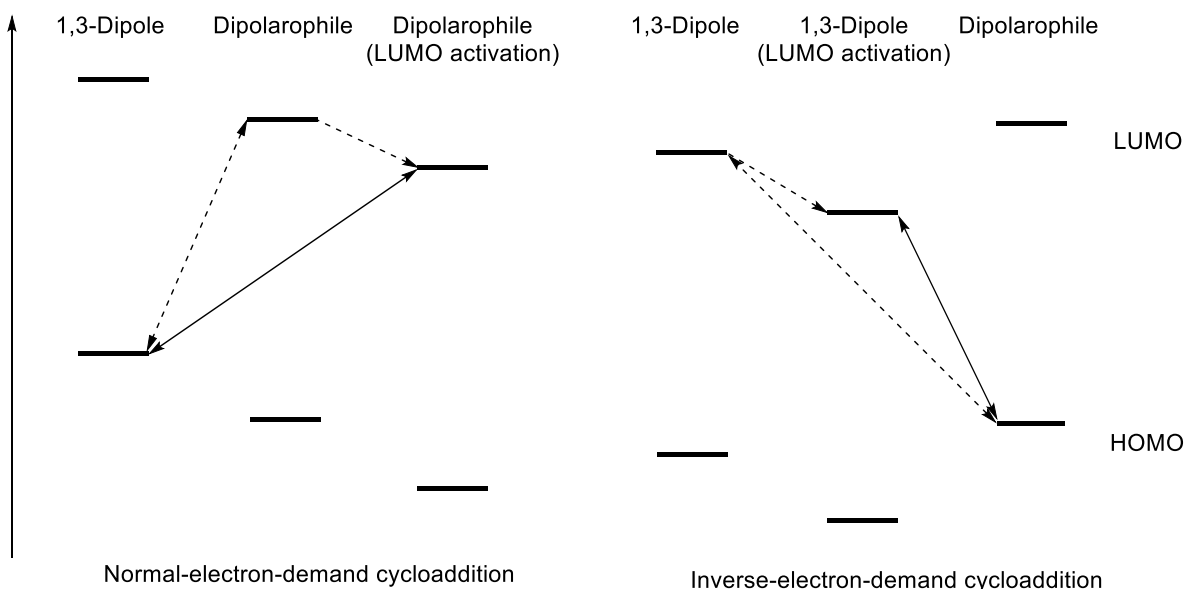
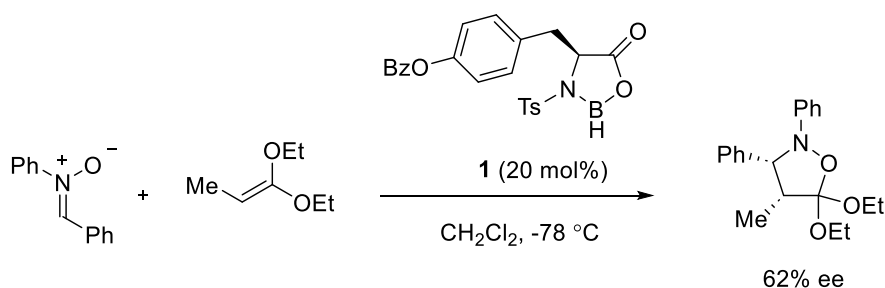


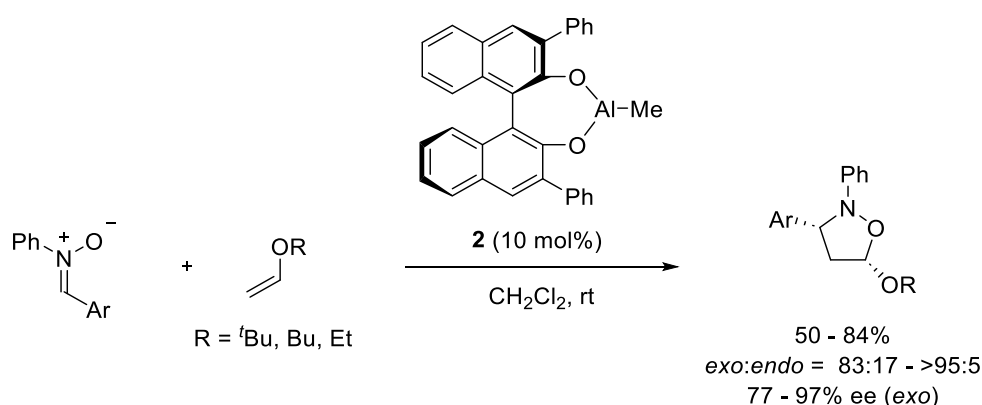
Figure 2. LUMO activation of normal- and inverse-electron-demand cycloadditions

2. NITRONE CYCLOADDITIONS

Although chiral oxazaborolidines would be classified as Lewis acid catalysts rather than organocatalysts, Scheeren and co-workers reported the first catalytic asymmetric IED 1,3-dipolar cycloadditions of nitrones in 1994 (Scheme 1).⁷ The reaction between *C,N*-diphenylnitronone and a ketene acetal in the presence of tyrosine-derived oxazaborolidine **1** afforded a cycloadduct with modest enantioselectivity. Successful examples of catalytic asymmetric IED 1,3-dipolar cycloadditions of nitrones have been limited, even including chiral Lewis acid catalysis. In 1999, Jørgensen and co-workers reported chiral Lewis acid-catalyzed asymmetric 1,3-dipolar cycloadditions of nitrones and vinyl ethers with the use of chiral Al-complex **2** composed of Me₃Al and 3,3'-diphenylbinaphthol, providing *exo*-cycloadducts with high diastereo- and enantioselectivities (Scheme 2).⁸ Cycloadditions of highly electron-deficient nitrones with vinyl ethers using a Cu(II)/chiral *t*-butyl-bisoxazoline complex were also reported to give *exo*-cycloadducts with good enantioselectivities.⁹



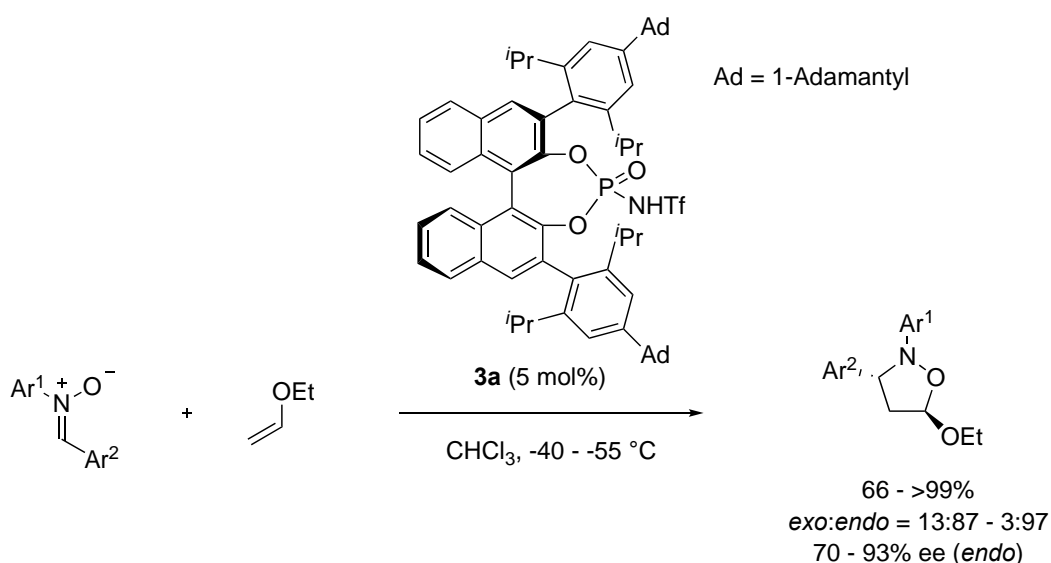
Scheme 1. Chiral oxazaborolidine-catalyzed asymmetric cycloaddition of nitronone



Scheme 2. Chiral Al-complex-catalyzed asymmetric cycloaddition of nitronone

In 2008, Yamamoto and co-workers reported a chiral *N*-triflylphosphoramidate as an organocatalyst that enabled *endo*-selective cycloaddition between nitrones and ethyl vinyl ether with high to good enantioselectivities.¹⁰ The cycloadditions between *C,N*-diarylnitrones (*Z*-nitrones) and ethyl vinyl ether in

the presence of 5 mol% of chiral *N*-triflylphosphoramidate **3a** in CHCl₃ at -40 – -50 °C afforded *endo*-cycloadducts with good to high enantioselectivities. In contrast to the chiral Lewis acid-catalyzed cycloadditions, the difference in the diastereoselectivity can be rationalized by transition state structures. The Brønsted acid catalysis, in which the acidic site (proton) is much smaller than that for Lewis acids (metal center), allows ethyl vinyl ether to selectively approach the nitron from the *endo*-direction. In addition, hydrogen bonding between the proton and the oxygen atom of ethyl vinyl ether may favor the *endo*-approach, while the *exo*-approach might be disfavored because of the steric repulsion between the ethoxy and R² groups (Figure 3). This report is a seminal work for organocatalytic asymmetric IED 1,3-dipolar cycloadditions.



Scheme 3. Asymmetric cycloaddition of nitron using chiral *N*-triflylphosphoramidate

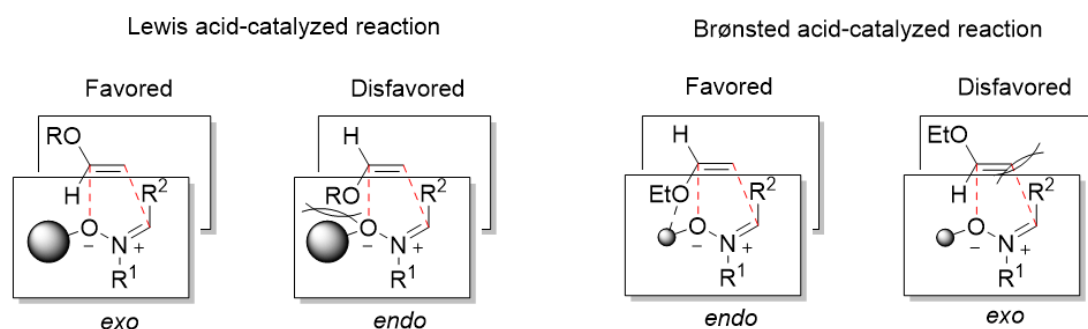
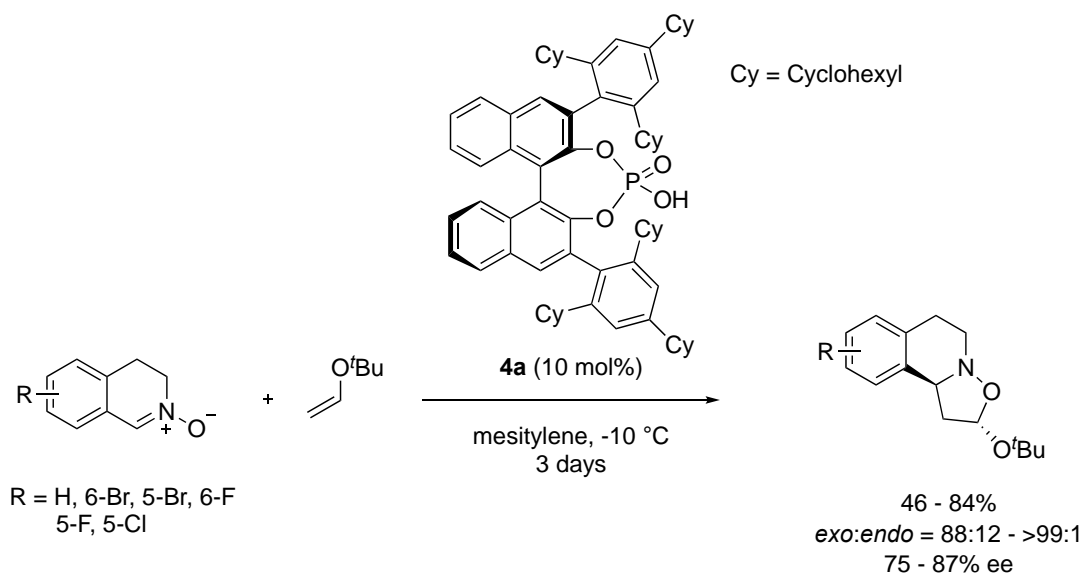


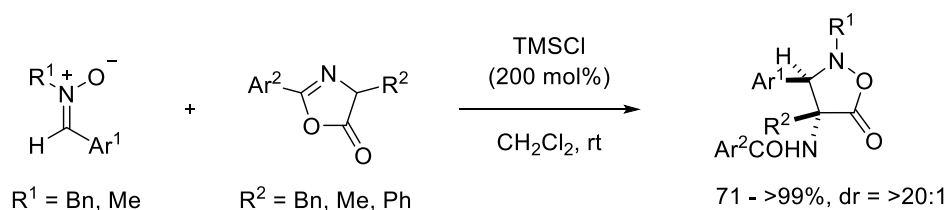
Figure 3. Transition-state structures showing diastereoselectivity of cycloaddition of nitron

In 2019, Akiyama and co-workers reported an asymmetric cycloaddition of tetrahydroisoquinoline-derived nitrones with *t*-butyl vinyl ether using chiral phosphoric acid **4a** (Scheme 4).¹¹ In this case, *exo*-cycloadducts were obtained with high diastereoselectivity and good enantioselectivity. The high *exo*-selectivity was probably due to the use of an *E*-nitron, which disfavored the *endo*-approach by steric

hindrance of the *t*-butoxy group of the vinyl ether. The reaction of the electron-rich cyclic nitron with 6,7-dimethoxy groups did not proceed under standard conditions.



Scheme 4. Asymmetric cycloaddition of cyclic nitron using chiral phosphoric acid



Scheme 5. TMSCl-promoted [3+2] cycloaddition between nitron and oxazol-5(4*H*)-ones

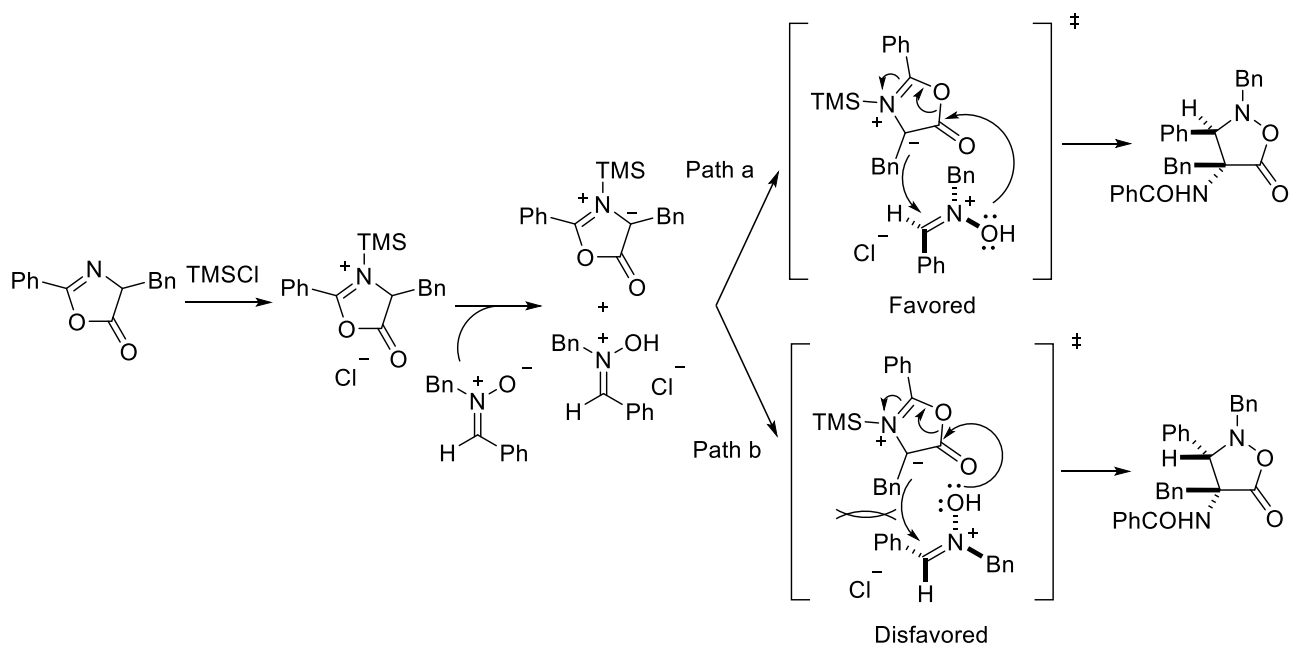
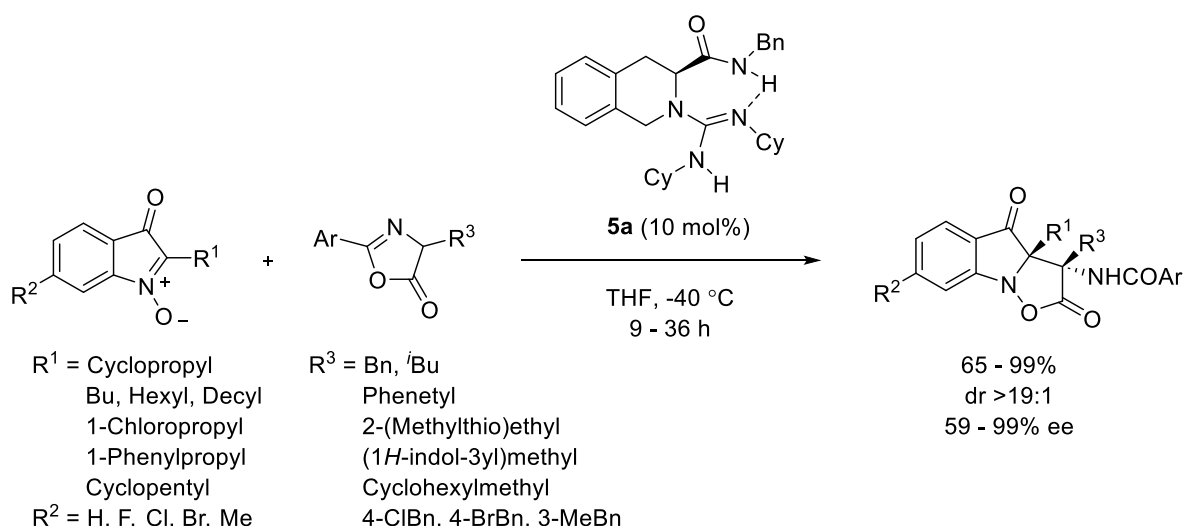


Figure 4. Proposed mechanism for the high diastereoselectivity of TMSCl-promoted [3+2] cycloadditions

In 2016, Zhao and co-workers reported TMSCl-promoted diastereoselective [3+2] cycloaddition between nitrones and oxazol-5(4*H*)-ones to furnish isoxazolidin-5-ones in reasonable chemical yields (Scheme 5).¹² The proposed mechanism for formation of isoxazolidin-5-ones was via deprotonation of *N*-silylated oxazol-5(4*H*)-one by a nitron as a base followed by a cascade nucleophilic addition-ring closure process (Figure 4). The high diastereoselectivity was explained by strong steric repulsion between the alkyl group of the oxazol-5(4*H*)-one and the *C*-aryl group of the nitron. Although the [3+2] cycloaddition seems to proceed through a stepwise pathway, the reaction could be classified as an IED cycloaddition based on the LUMO_{dipole}-HOMO_{dipolarophile} interaction. Use of combined catalysis by TMSCl (10 mol%) and organocatalysts (10 mol%) such as a quinine-based squaramide, cyclohexanediamine-derived thiourea, and a silylated prolinol derivative, resulted in no asymmetric induction.

In 2021, Liu and co-workers reported asymmetric formal [3+2] cycloaddition of indolone-*N*-oxides with oxazol-5(4*H*)-ones using chiral amide-guanidine **5a** with high diastereoselectivity and enantioselectivity (Scheme 6).¹³ The high diastereoselectivity was explained by the favorable *rel-Re-Si* attack of the two components, which favors the attack of the oxazol-5(4*H*)-one by the oxygen atom, while the *rel-Re-Re* interaction is disfavored due to steric hindrance or the far-attack of the oxazol-5(4*H*)-one by the oxygen atom (Figure 5). A bifunctional activation mode was proposed to rationalize the enantioselection of the reaction, in which the amide unit provides a hydrogen bond to interact with the oxygen atom of the N-O bond in the nitron. The basic guanidine unit accelerates enolization of the oxazol-5(4*H*)-one, and then, the *Re*-face of the enolate intermediate approaches the nitron from its *Si*-face.



Scheme 6. Asymmetric [3+2] cycloaddition with oxazol-5(4*H*)-ones using chiral amide-guanidine

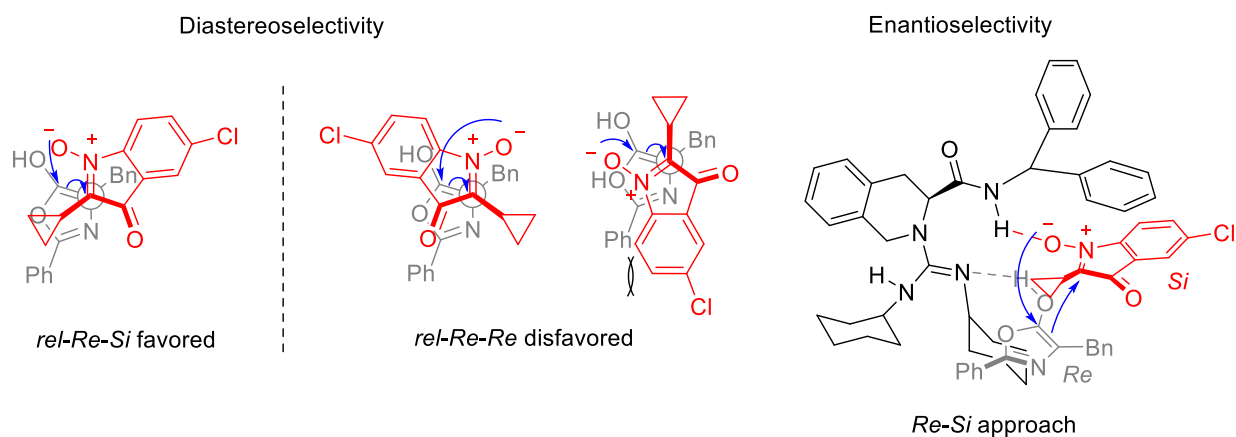
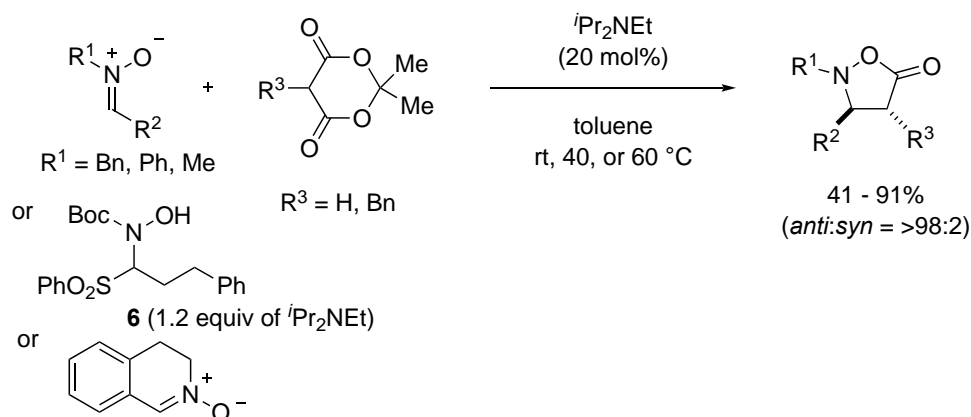
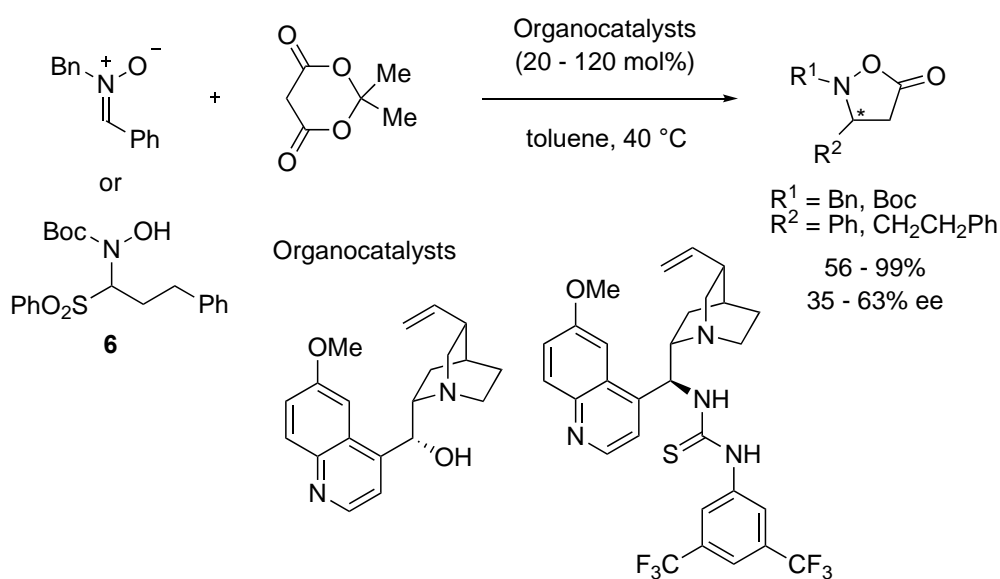


Figure 5. Proposed working model for asymmetric formal [3+2] cycloaddition



Scheme 7. Domino anionic formal [3+2] cycloaddition-decarboxylation reactions of nitronium with Meldrum's acid



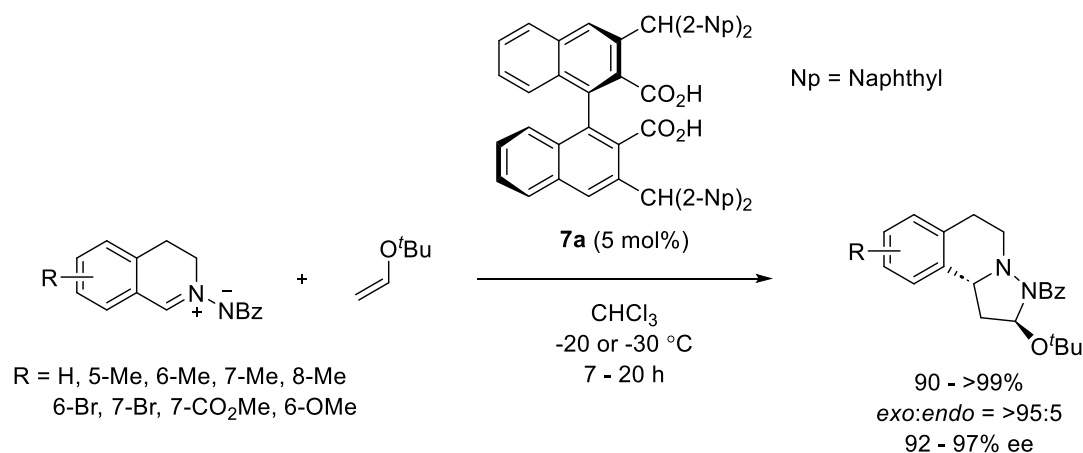
Scheme 8. Enantioselective approach for formal [3+2] cycloaddition-decarboxylation reactions

Domino anionic formal [3+2] cycloaddition-decarboxylation reactions of nitrones with Meldrum's acid under mild Brønsted basic conditions were reported by Brière and co-workers (Scheme 7).¹⁴ In the organocatalytic reactions, Meldrum's acid acted as a useful ketene equivalent to afford isoxazolidin-5-one derivatives. The first asymmetric version of this reaction with moderate enantioselectivity was demonstrated by means of quinine-based organobase catalysts using *C*-phenyl-*N*-benzyl nitron or its *N*-Boc nitron precursor **6** (Scheme 8).

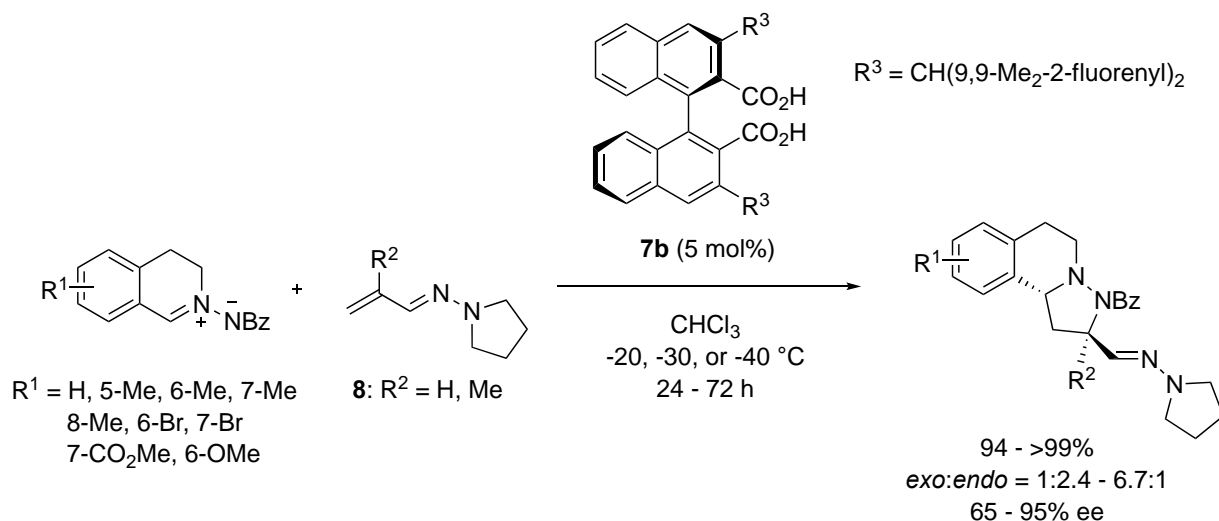
3. AZOMETHINE IMINE CYCLOADDITIONS

3-1. *C,N*-CYCLIC AZOMETHINE IMINE CYCLOADDITION

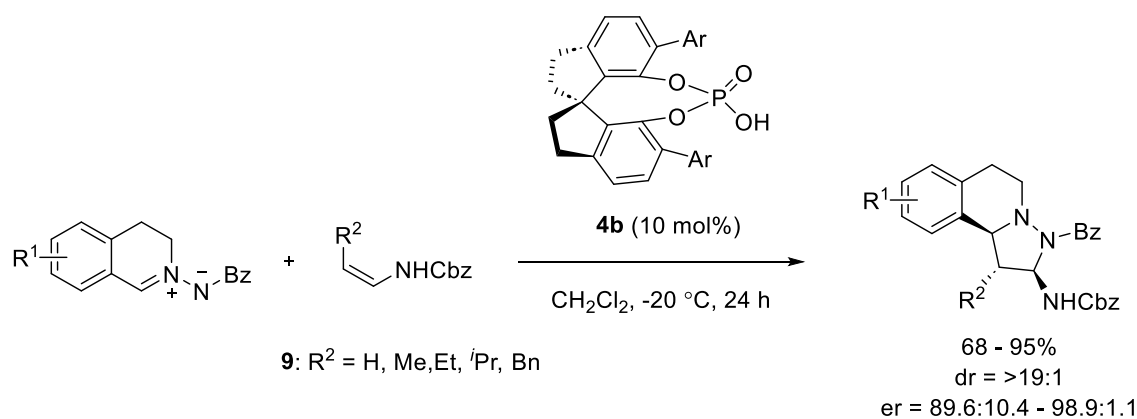
The asymmetric IED 1,3-dipolar cycloaddition between *C,N*-cyclic azomethine imines and *t*-butyl vinyl ether using chiral dicarboxylic acids as a class of chiral Brønsted acid catalysts was first reported by Maruoka, Hashimoto, and co-workers in 2011 (Scheme 9).¹⁵ The use of axially chiral binaphthyl dicarboxylic acid **7a** bearing di(2-naphthyl)methyl groups at the 3,3'-positions in the reaction of tetrahydroisoquinoline-based *C,N*-cyclic azomethine imines in CHCl₃ at -20 or -30 °C provided the best result in terms of enantioselectivity (92 – 97% ee) with high yield and diastereoselectivity. Vinylogous azanamines **8** as electron-rich dipolarophiles were also employed for this catalytic system using a modified dicarboxylic acid **7b** bearing bis(9,9-dimethyl-2-fluorenyl)methyl groups at the 3,3'-positions (Scheme 10). Enecarbamates **9** could be used as dipolarophiles in the asymmetric IED 1,3-dipolar cycloaddition of tetrahydroisoquinoline-based *C,N*-cyclic azomethine imines in the presence of chiral phosphoric acid **4b**, which was reported by Zhu and co-workers in 2016 (Scheme 11).¹⁶ In contrast to high *exo*-selectivity provided by chiral dicarboxylic acid-catalyzed cycloaddition of *C,N*-cyclic azomethine imines with *t*-butyl vinyl ether, high *endo*-selectivity with high enantioselectivity was observed.



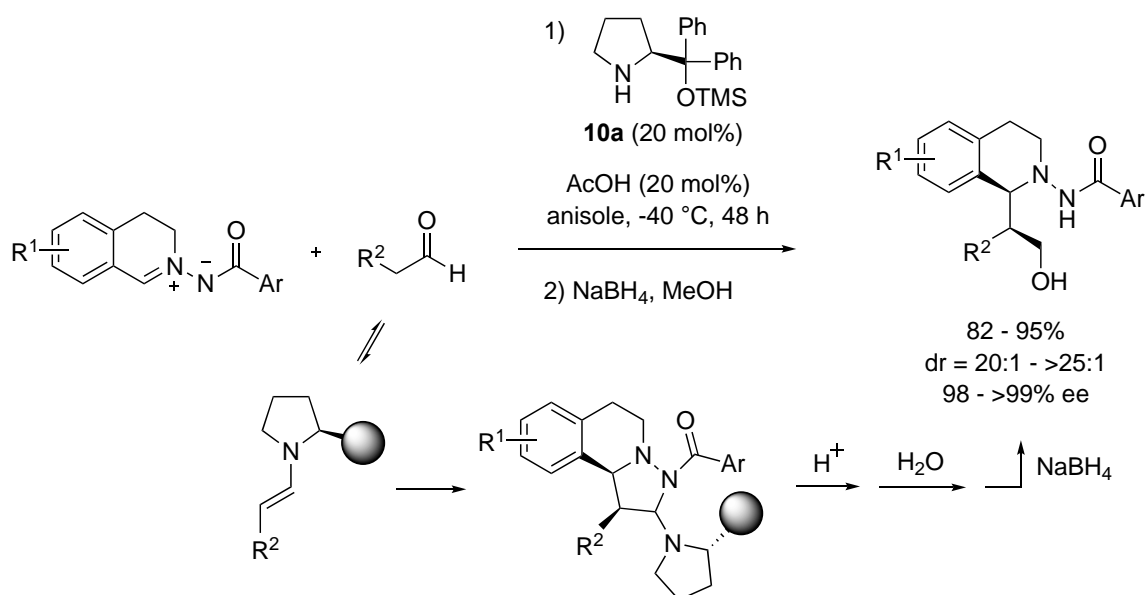
Scheme 9. Asymmetric cycloaddition between *C,N*-cyclic azomethine imines and *t*-butyl vinyl ether using chiral dicarboxylic acids



Scheme 10. Asymmetric cycloaddition with vinylogous aza-enamines

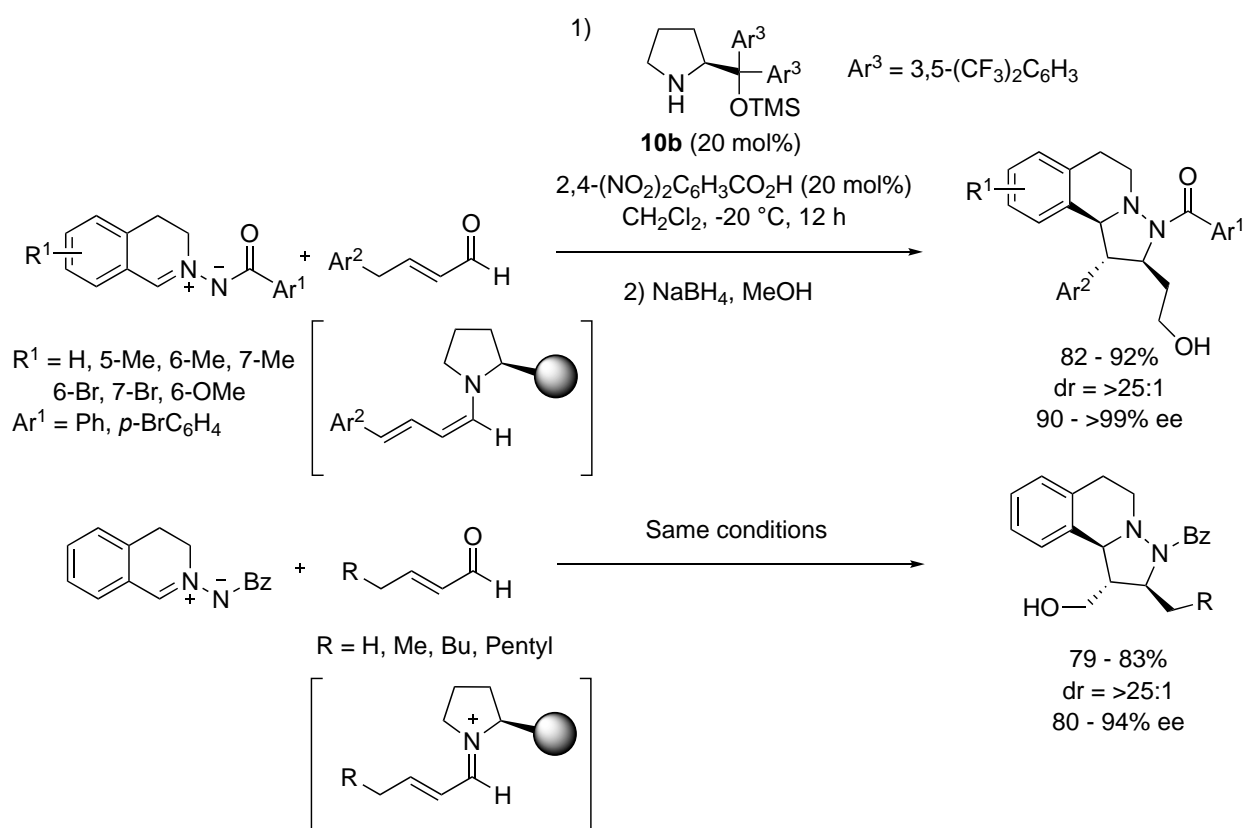


Scheme 11. Asymmetric cycloaddition with enecarbamates

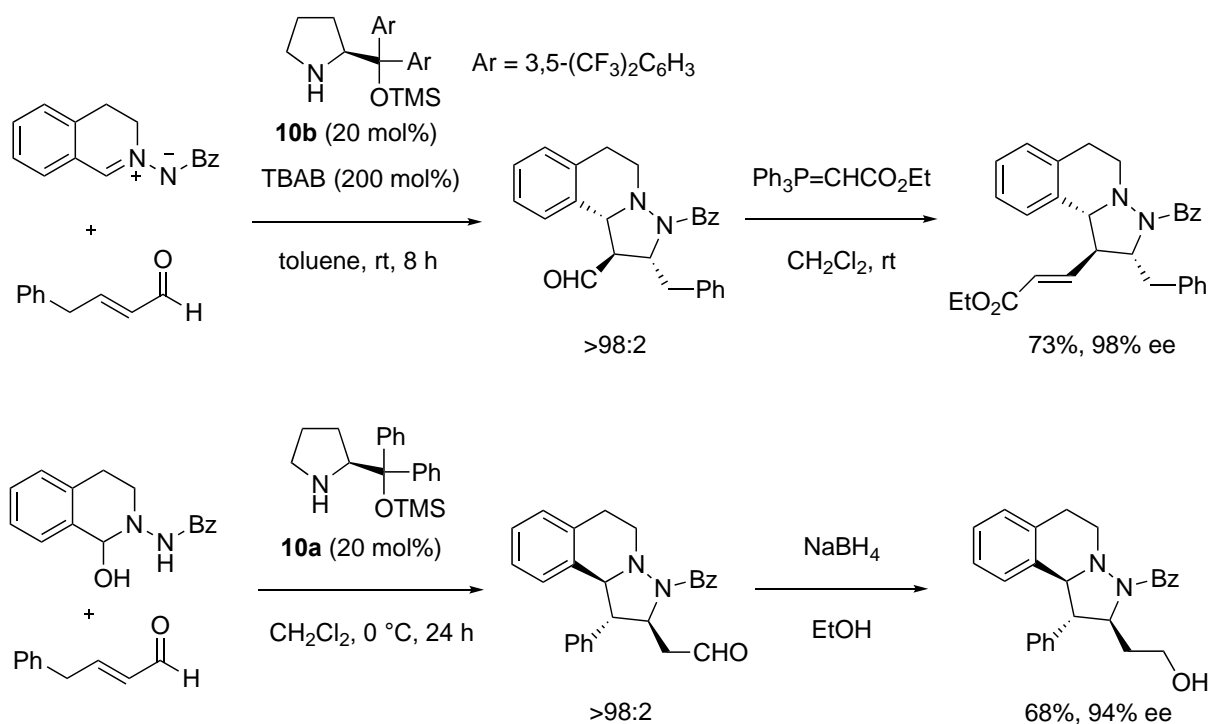


Scheme 12. Chiral amine-catalyzed enantioselective 1,3-dipolar cycloaddition with aldehydes

In 2014, Wang and co-workers reported chiral amine-catalyzed asymmetric 1,3-dipolar cycloaddition of *C,N*-cyclic azomethine imines, in which TMS-protected chiral prolinol catalyst **10a** generated chiral enamines from aldehydes (Scheme 12).¹⁷ The cycloaddition reaction using tetrahydroisoquinoline-based *C,N*-cyclic azomethine imines in anisole could be promoted by addition of AcOH (20 mol%) to give aza-acetal cycloadducts, which were converted *in situ* to more stable hydrazide derivatives by reduction with sodium borohydride in MeOH. The corresponding products were obtained in high yields with high enantio- and diastereoselectivities. In the same year, Du, Wang, and co-workers reported a dienamine-mediated enantioselective 1,3-dipolar cycloaddition between tetrahydroisoquinoline-based *C,N*-cyclic azomethine imines and α,β -unsaturated aldehydes (Scheme 13).¹⁸ In this case, the highest enantioselectivity was obtained with the use of (*S*)-bis[3,5-bis(trifluoromethyl)phenyl]pyrrolidine catalyst **10b** (20 mol%) and 2,4-dinitrobenzoic acid (20 mol%) in CH₂Cl₂ at -20 °C. For α,β -unsaturated aldehydes bearing aromatic substituents including heterocycles on the side chain, the cycloaddition proceeded in an IED manner through dienamine intermediates with high enantio- and diastereoselectivity. Conversely, aliphatic α,β -unsaturated aldehydes underwent NED 1,3-dipolar cycloaddition to furnish the corresponding products with good to high enantioselectivity and high diastereoselectivity.



Scheme 13. Dienamine-mediated enantioselective 1,3-dipolar cycloaddition with α,β -unsaturated aldehydes



Scheme 14. Control of dual reactivity of β -arylmethyl α,β -unsaturated aldehydes

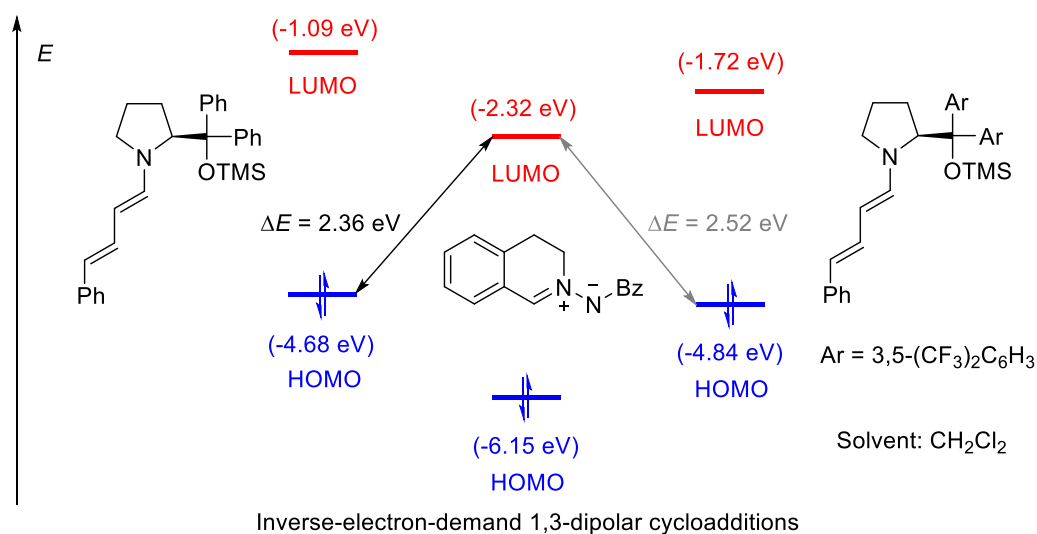


Figure 6. FMO energies calculated for azomethine imine and iminium ions (IED 1,3-dipolar cycloaddition)

Alemán, Fraile, and co-workers investigated the dual reactivity of β -arylmethyl α,β -unsaturated aldehydes in organocatalytic 1,3-dipolar cycloadditions with *N*-benzoyl *C,N*-cyclic azomethine imines (Scheme 14).¹⁹ Interestingly, the chemoselectivity (iminium ion vs. dienamine) was found to be completely controlled by the catalysts and additives. For example, the cycloadduct derived from an iminium ion intermediate was afforded with high chemo- and enantioselectivity by using (*S*)-bis[3,5-bis(trifluoromethyl)phenyl]-pyrrolidine **10b** and tetrabutylammonium bromide (TBAB) in toluene in the reaction of *N*-benzoyl *C,N*-

cyclic azomethine imine with 4-phenyl-2-butenal. In contrast, the cycloadduct derived from a dienamine intermediate was obtained with high chemo- and enantioselectivity by using (*S*)-diphenylpyrrolidine **10a** without an additive in CH₂Cl₂ in the reaction of the hydrated *N*-benzoyl *C,N*-cyclic azomethine imine. The chemoselectivity switch by organocatalysts and solvents was satisfactorily explained by DFT calculations for the HOMO_{dienamine}-LUMO_{dipole} and HOMO_{dipole}-LUMO_{iminium} interactions according to Sustmann-Huisgen type analysis (Figures 6 and 7).

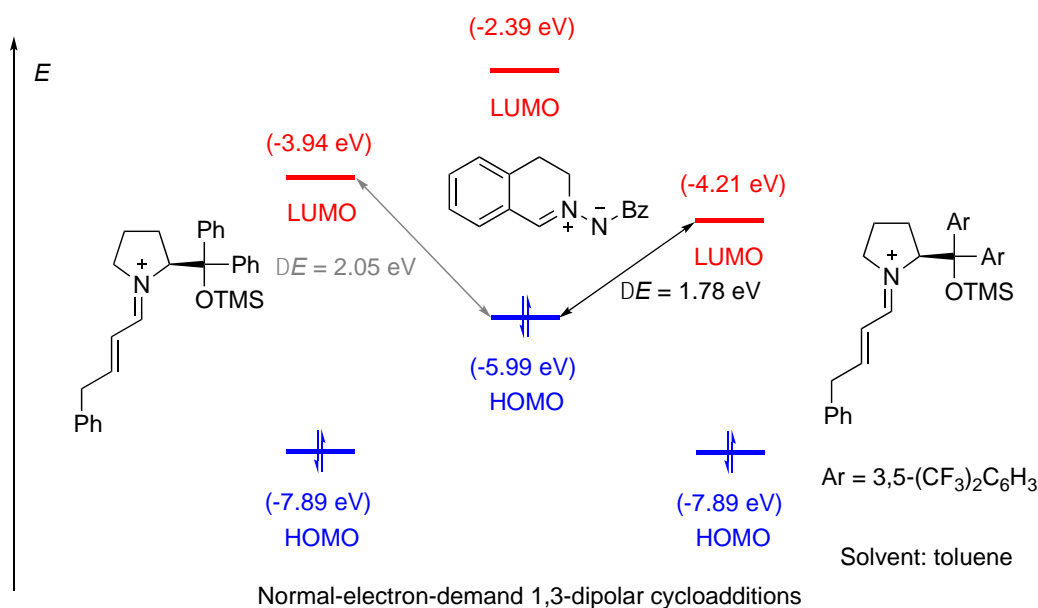
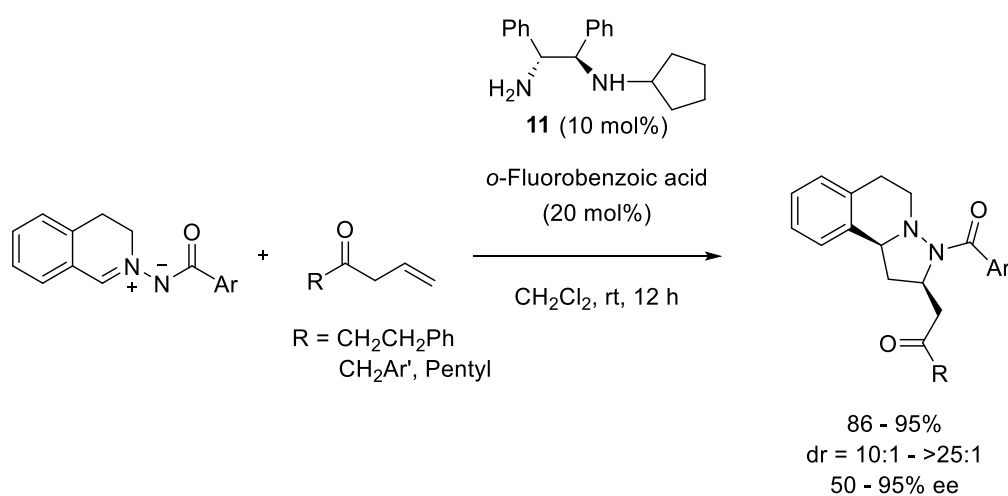
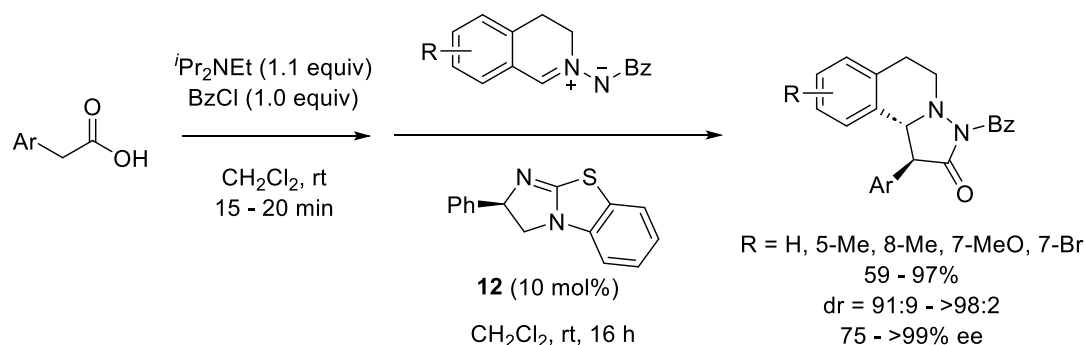


Figure 7. FMO energies calculated for azomethine imine and dienamines (NED 1,3-dipolar cycloaddition)



Scheme 15. Asymmetric cycloaddition with allyl alkyl ketones

In 2021, K. Wang, S. Wang, and co-workers reported the catalytic asymmetric 1,3-dipolar cycloaddition reaction between tetrahydroisoquinoline-based *C,N*-cyclic azomethine imines and allyl alkyl ketones through dienamine intermediates using chiral primary amine **11** (Scheme 15).²⁰ The reaction tolerated a wide range of functional groups in terms of the *N*-acyl substituent of azomethine imines and the alkyl substituent of allyl alkyl ketones, affording an array of tetrahydroisoquinoline derivatives with good diastereo- and enantioselectivities.



Scheme 16. Chiral Lewis base-catalyzed formal [3+2] cycloaddition with mixed anhydrides

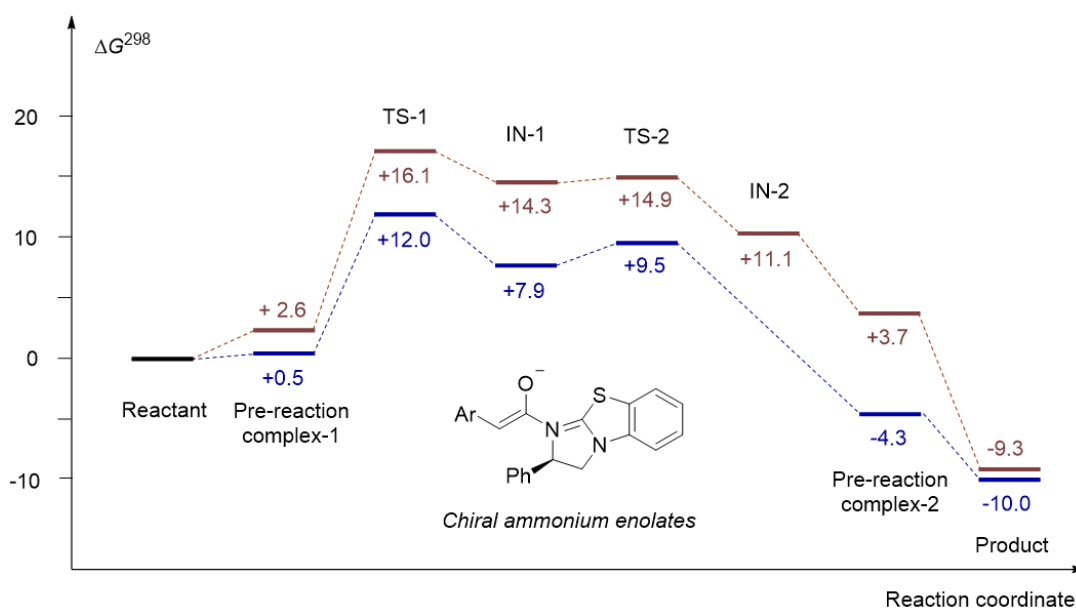
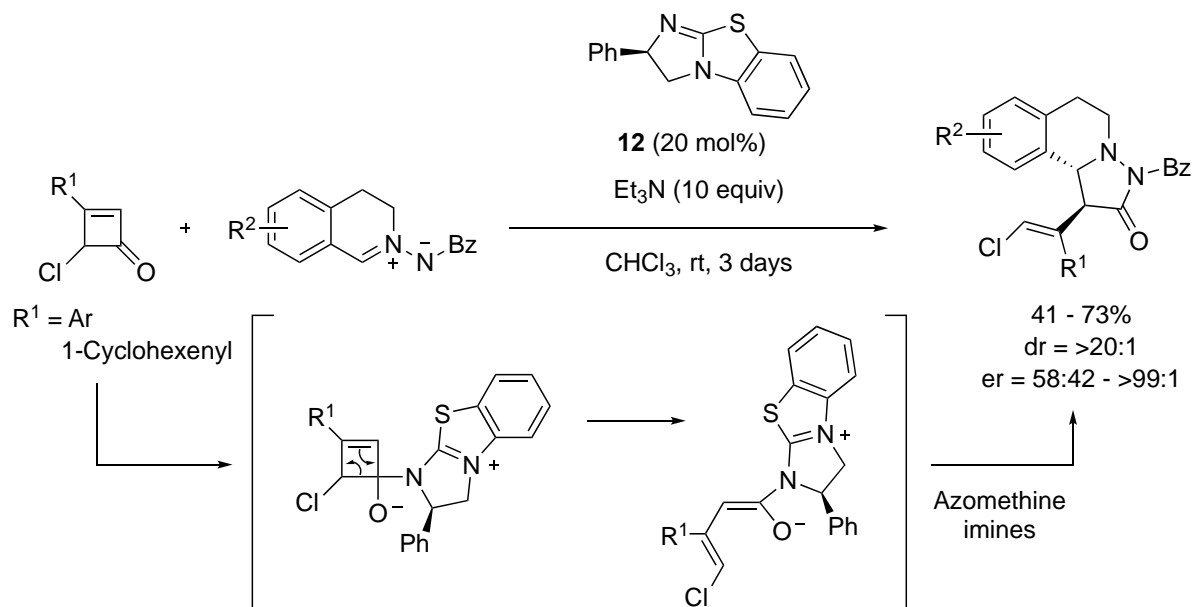


Figure 8. Chemical structure of chiral ammonium enolates and DFT calculated free energies of cycloaddition

In 2015, Mück-Lichtenfeld, Studer, and co-workers reported a chiral Lewis base-catalyzed asymmetric formal [3+2] cycloaddition between tetrahydroisoquinoline-based *C,N*-cyclic azomethine imines and mixed anhydrides with high diastereo- and enantioselectivities (Scheme 16).²¹ The mixed anhydrides were generated *in situ* from the corresponding arylacetic acids and benzoyl chloride, and then the reaction with

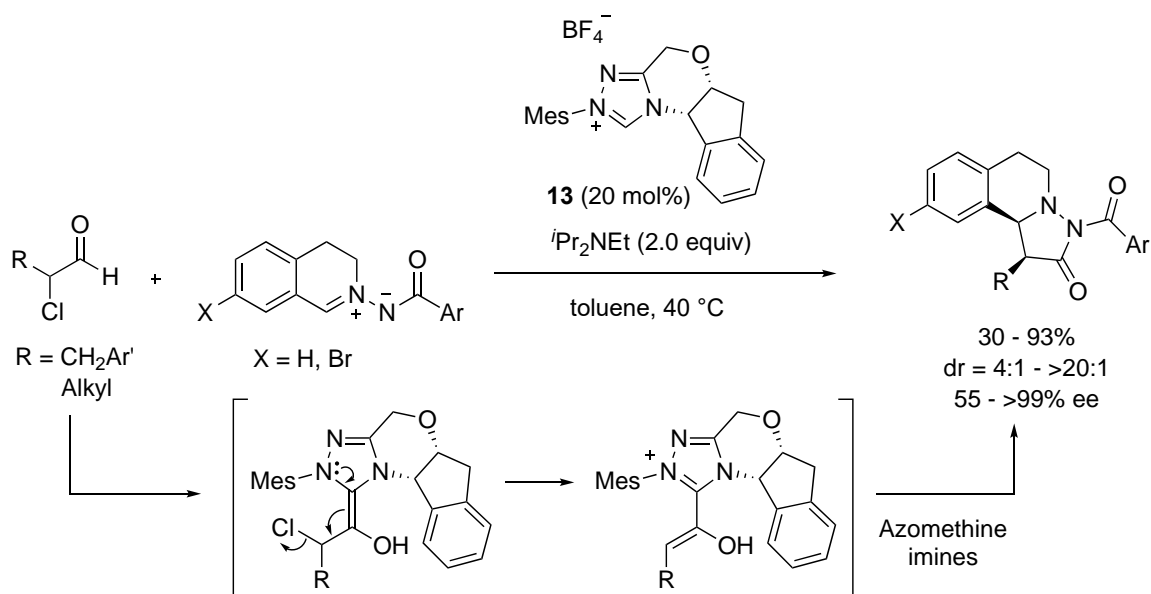
isothiourea-type chiral Lewis base **12** afforded chiral ammonium enolates that acted as dipolarophiles. By theoretical studies of the mechanism using DFT calculations, the cycloaddition was found to proceed stepwise via C-C bond formation followed by C-N bond formation with a very low energy barrier. The first step is the rate- and stereo-determining step, in which the preferable orientation of the two reactants in the pre-reactive complex reflects the stereochemical outcome (Figure 8).

In 2015, Chi and co-workers reported a chiral isothiourea-catalyzed asymmetric cycloaddition of *C,N*-cyclic azomethine imines using a γ -monochloride-substituted cyclobutanone (Scheme 17).²² The dienolate catalyst-bound intermediate was generated by the reaction of chiral isothiourea **12** along with C-C bond cleavage. The catalytically-generated intermediate as a dipolarophile underwent an α -carbon selective reaction with the azomethine imines to afford pyrazolidinone derivatives with mostly high diastereo- and enantioselectivities.

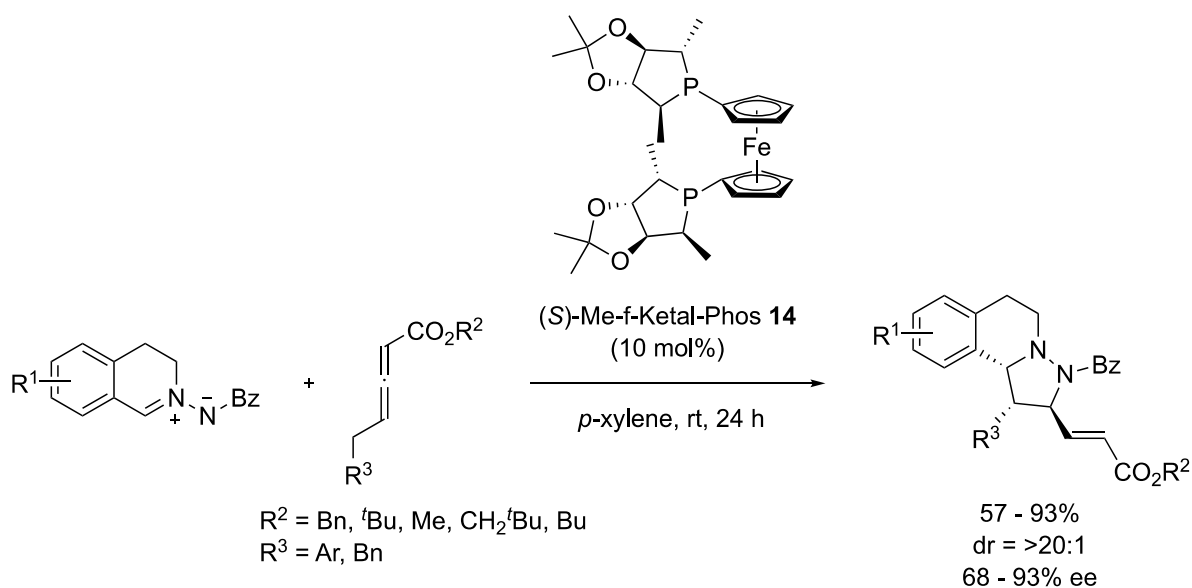


Scheme 17. Chiral isothiourea-catalyzed asymmetric cycloaddition using a γ -monochloride-substituted cyclobutanone

An *N*-heterocyclic carbene-catalyzed enantioselective [2+3] cyclocondensation of α -chloroaldehydes with azomethine imines was developed by Liao, Ye, and co-workers (Scheme 18).²³ Similar types of pyrazolidinone derivatives were provided in good yield with moderate to good diastereoselectivity and high enantioselectivity. In contrast to Studer's work in which only β -aryl carboxylic acids were employed, both β -aryl and β -alkyl α -chloroaldehydes were applicable in this reaction using triazolium salt **13** as an *N*-heterocyclic carbene precursor.



Scheme 18. *N*-Heterocyclic carbene-catalyzed enantioselective [2+3] cyclocondensation of α -chloroaldehydes



Scheme 19. Chiral phosphine-catalyzed asymmetric [3+2] cycloaddition with δ -substituted allenoates

A chiral phosphine-catalyzed asymmetric [3+2] cycloaddition of *C,N*-cyclic azomethine imines with δ -substituted allenoates was developed by Shi and co-workers (Scheme 19).²⁴ The cycloaddition in the presence of 10 mol% of (*S*)-Me-f-Ketal-Phos **14** afforded functionalized tetrahydroquinoline derivatives in good yields with high diastereo- and good enantioselectivity under mild conditions. A plausible mechanism for this [3+2] cycloaddition was proposed based on a deuterium-labeling experiment (Figure 9). The novelty of the study is that this type of allenoate can be used as a δ,γ -C-C bond participated C2 synthon in the asymmetric cycloaddition.

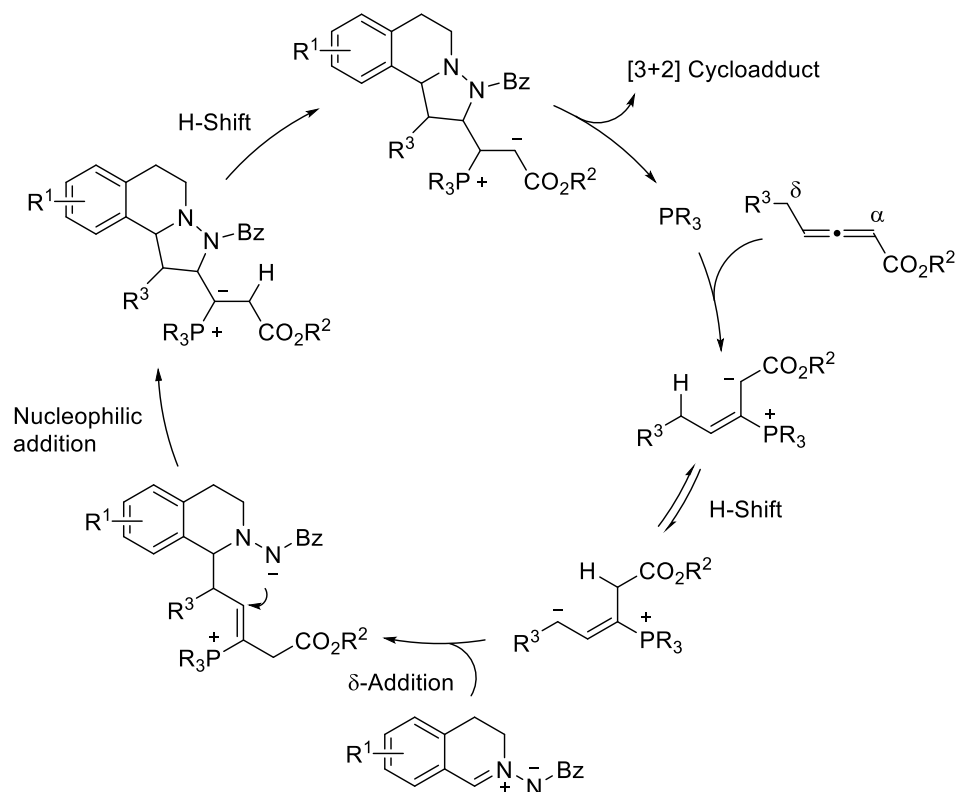
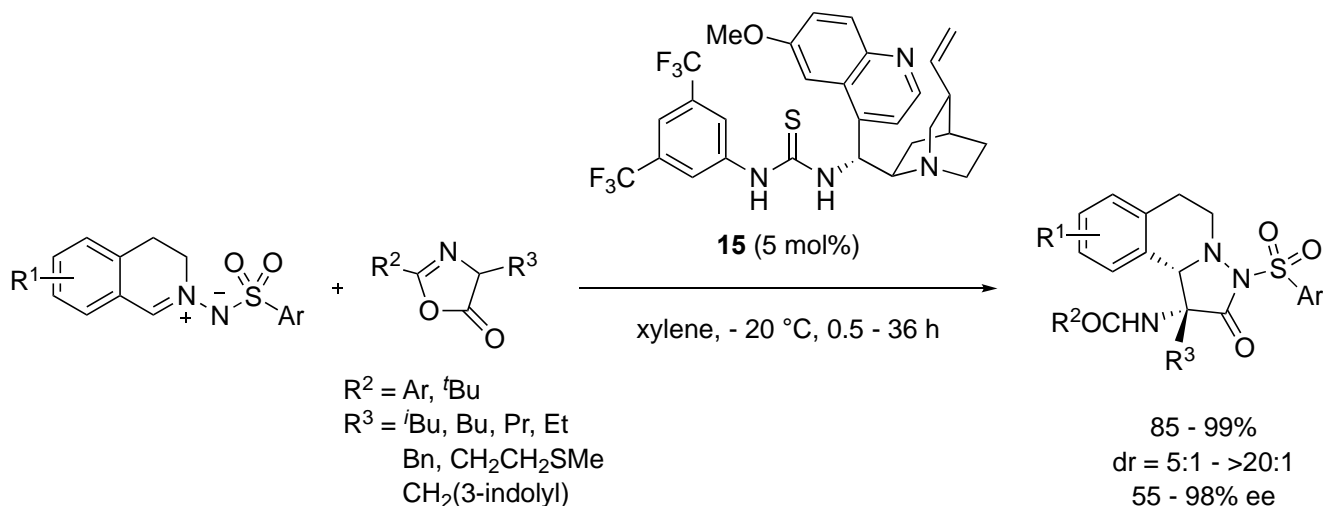


Figure 9. Plausible mechanism for [3+2] cycloaddition



Scheme 20. Bifunctional organocatalyst-mediated enantioselective cycloaddition with azlactones

Azlactones (oxazol-5(4*H*)-ones) could be used as dipolarophiles in the asymmetric IED 1,3-dipolar cycloaddition of *C,N*-cyclic azomethine imines, which was reported in 2016 by Liu, Su, and co-workers (Scheme 20).²⁵ This methodology using a bifunctional organocatalyst offers a novel scheme for the stereocontrolled synthesis of various C1-substituted tetrahydroisoquinolines bearing vicinal tertiary and azaquaternary stereocenters with high diastereo- and enantioselectivities. Under the catalysis of chiral amine-thiourea **15**, the *Re* face attack of the azlactone enolate to the *Re* face of the azomethine imine was

proposed for the transition states based on a double activation mode by a hydrogen-bonding interaction (Figure 10).

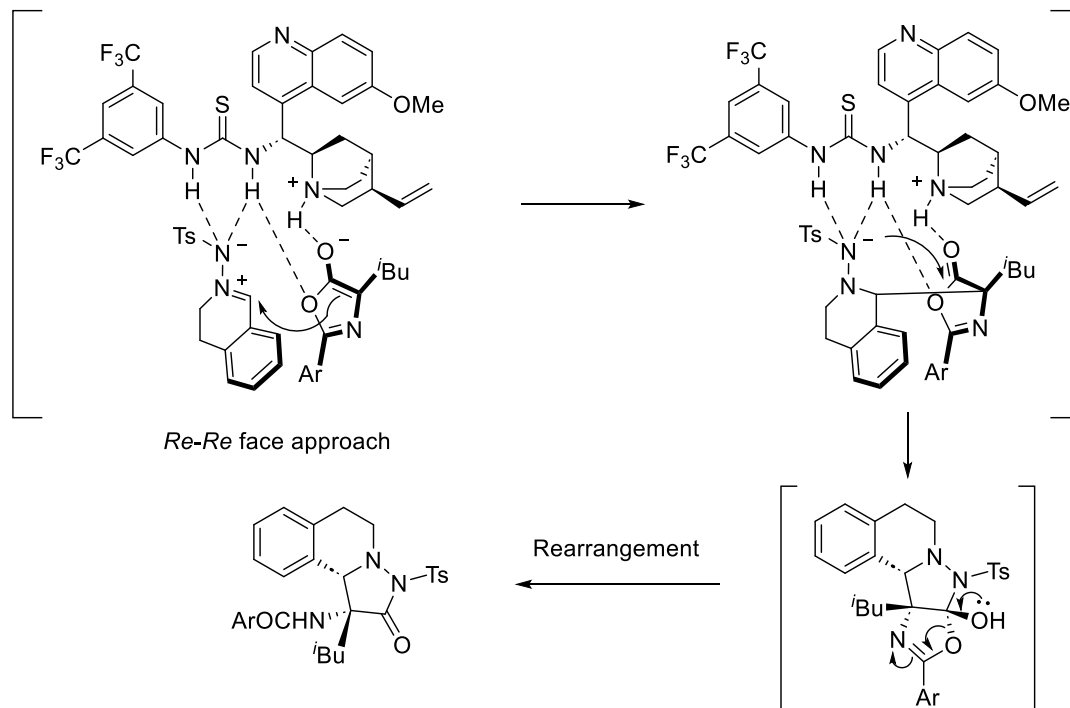
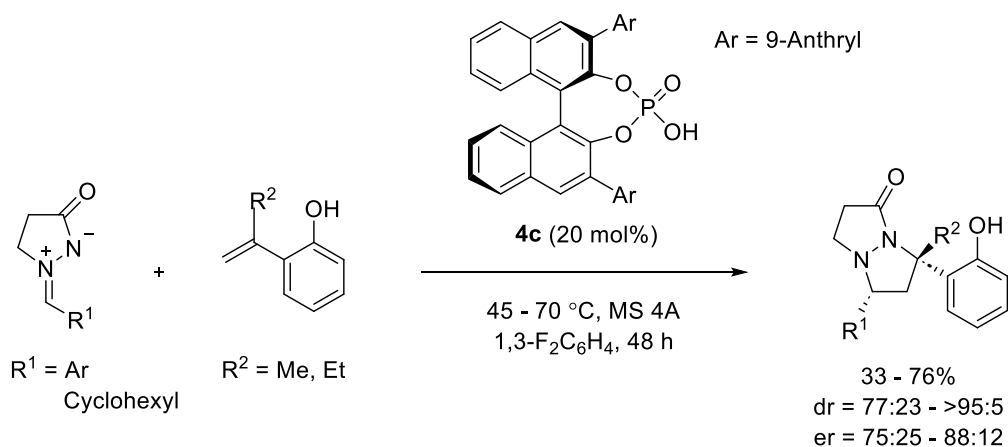


Figure 10. Proposed mechanism for transition states

3-2. *N,N*-CYCLIC AZOMETHINE IMINE CYCLOADDITION



Scheme 21. Asymmetric cycloaddition with *o*-hydroxystyrene derivatives in presence of chiral phosphoric acid

The first organocatalytic asymmetric IED 1,3-dipolar cycloaddition of *N,N'*-cyclic azomethine imines was established by the reaction with *o*-hydroxystyrene derivatives in the presence of chiral phosphoric acid **4c**

in 2014 by Shi and co-workers (Scheme 21).²⁶ Chiral *N,N*-bicyclic pyrazolidin-3-one derivatives with the creation of two stereogenic centers, one of which is quaternary, were provided by the cycloaddition with high diastereoselectivity and moderate enantioselectivity (up to >95:5 dr, 88:12 er). The authors suggested possible transition states to explain the stereoselectivity as shown in Figure 11.

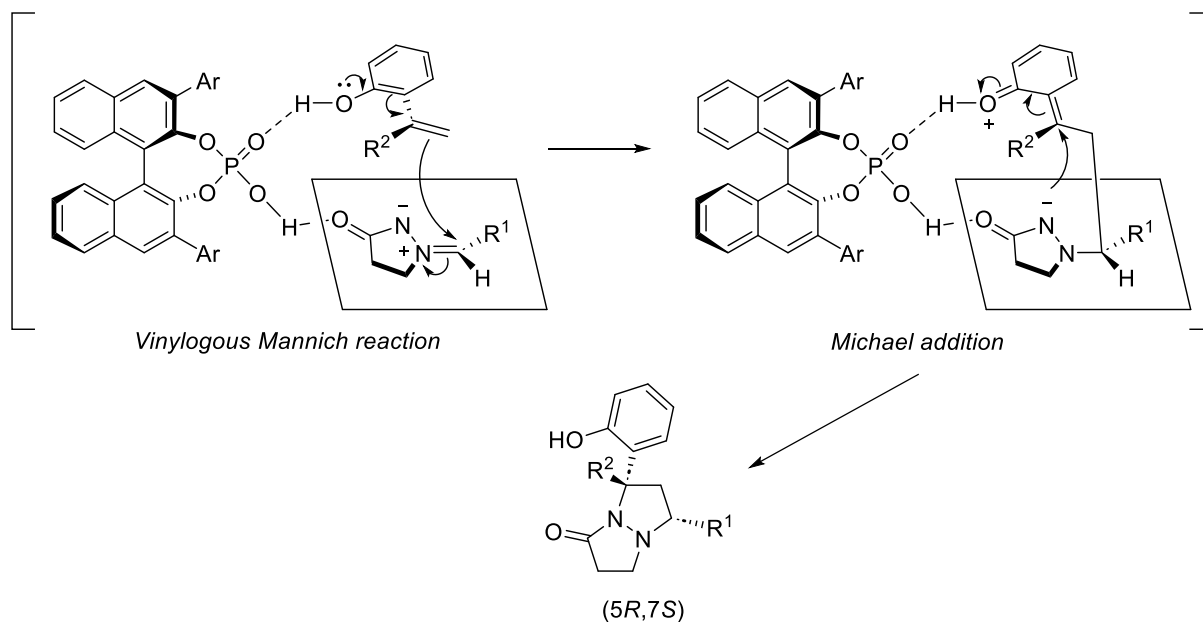
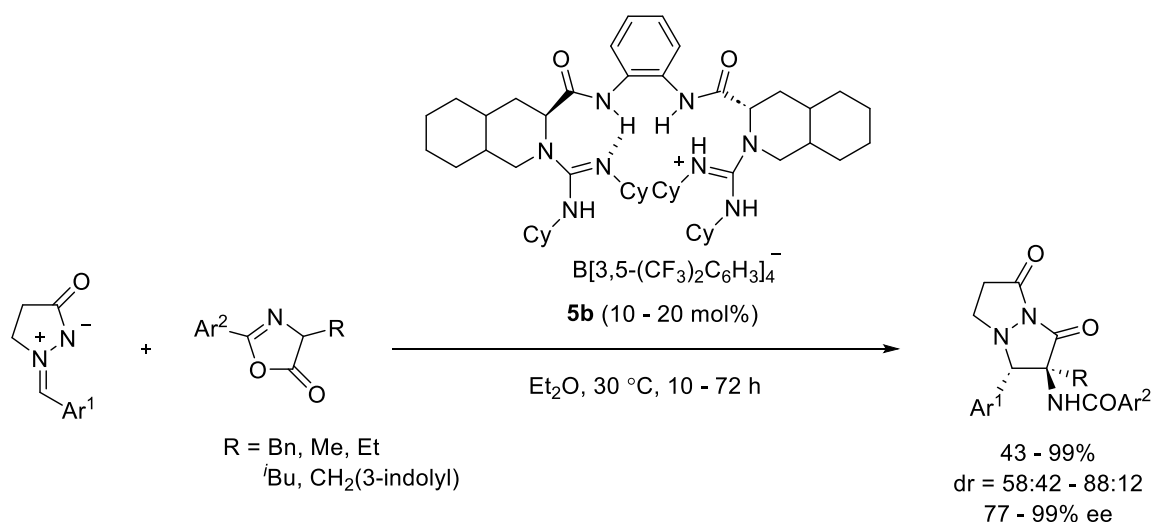


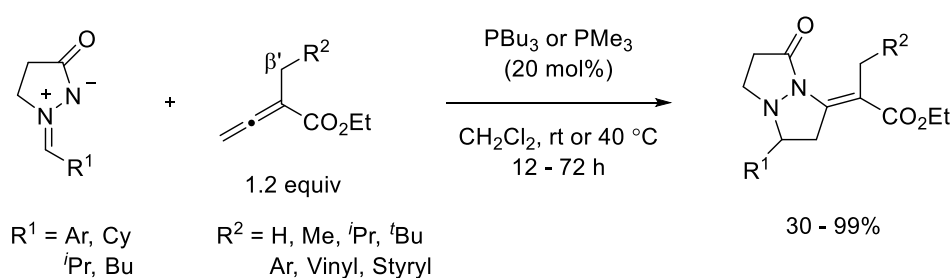
Figure 11. Proposed mechanism for transition states



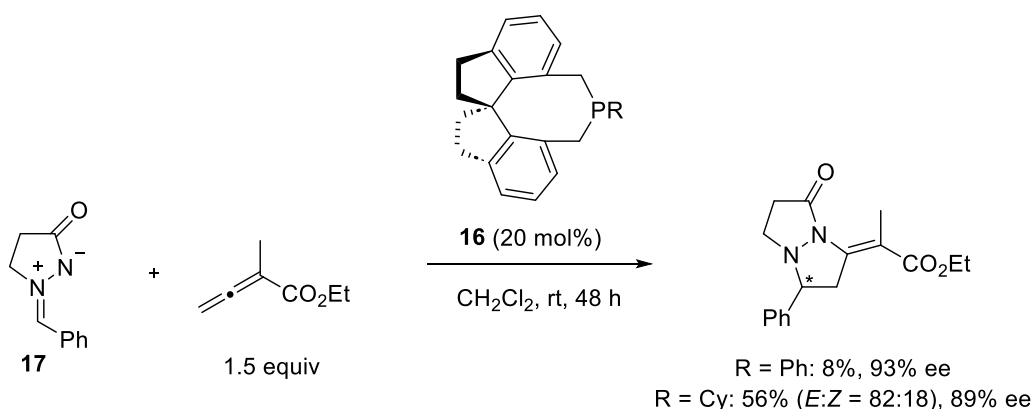
Scheme 22. Asymmetric formal [3+2] cycloaddition with azlactones using chiral bifunctional bisguanidinium hemisalt

In 2017, Liu and co-workers reported the asymmetric formal [3+2] cycloaddition of *N,N'*-cyclic azomethine imines with azlactones (oxazol-5(4*H*)-ones) using chiral bifunctional bisguanidinium hemisalt **5b** (Scheme

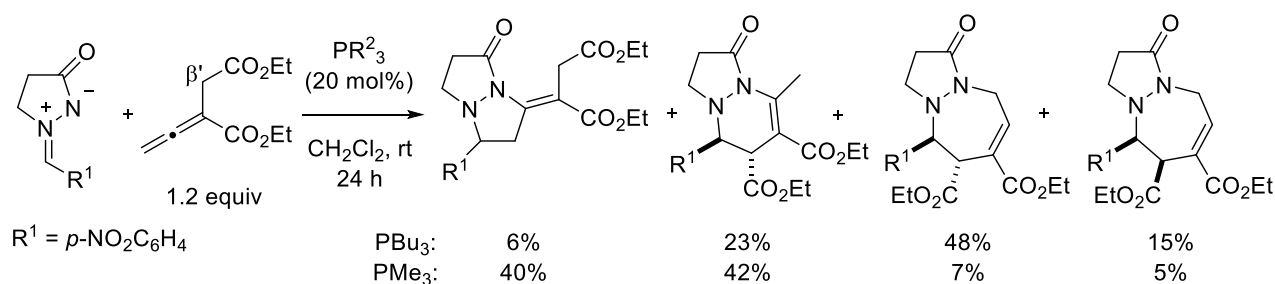
22).²⁷ Optically active bicyclic pyrazolidinone compounds bearing vicinal aza-quaternary and tertiary carbon centers were afforded in high yields with good diastereoselectivities and high ee values. Mechanistically, bisguanidinium hemisalt **5b** was proposed to promote the reaction as a bifunctional catalyst; one guanidine unit of the catalyst acts as a base to form the enolate intermediate from the azlactone, while the guanidinium salt interacts with the N-C=O portion of the dipole via hydrogen bonding to activate the azomethine imine.



Scheme 23. Phosphine-catalyzed [3+2] cycloaddition with allenates

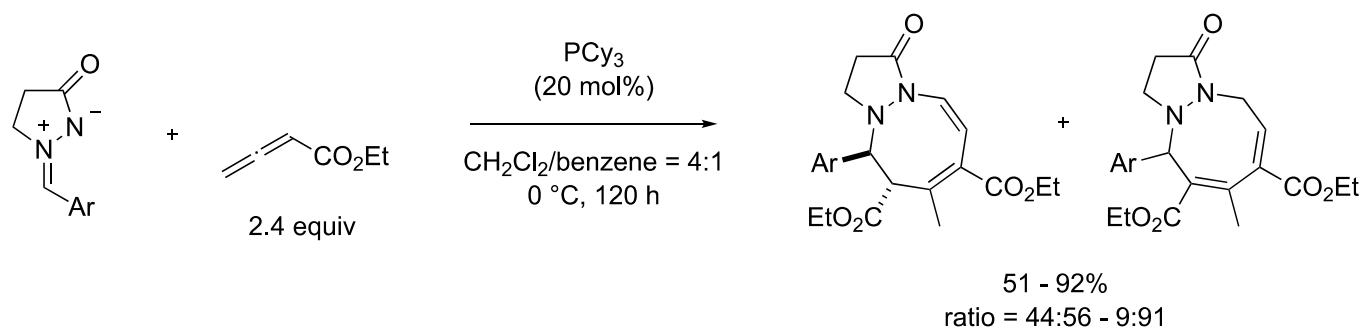


Scheme 24. Chiral spirophosphine-catalyzed asymmetric [3+2] cycloaddition

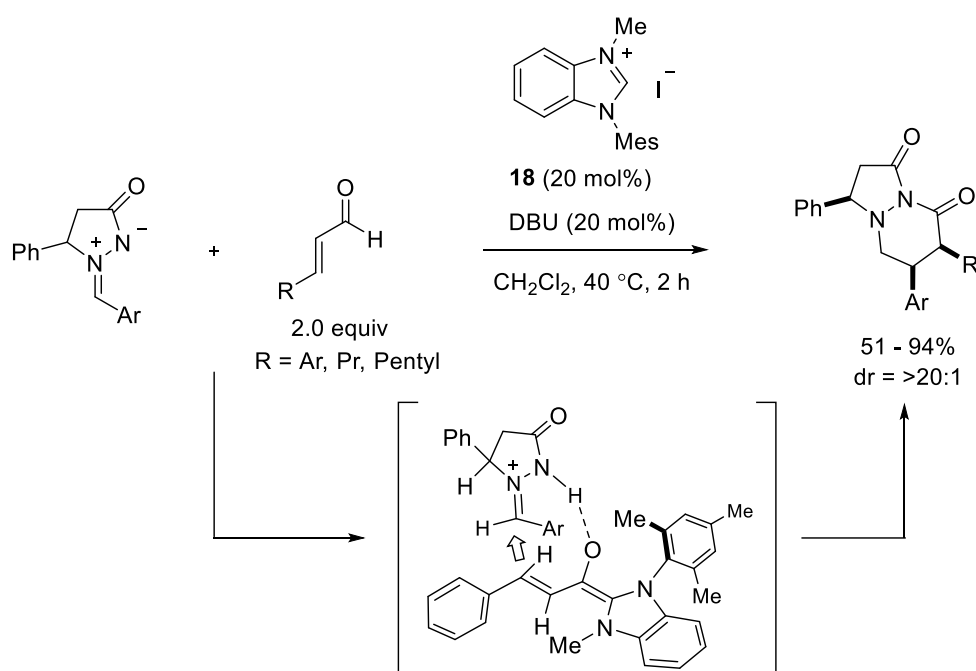


Scheme 25. Phosphine-catalyzed [3+2], [3+3], and [3+4] cycloadditions with diethyl 2-vinylidenesuccinate

A phosphine-catalyzed [3+2] cycloaddition of *N,N'*-cyclic azomethine imines with allenates was reported by Guo, Kwon, and co-workers in 2011 (Scheme 23).²⁸ Screening of tertiary phosphines for the catalysis revealed that the reactions using PBU_3 and PMe_3 led to good yields of the cycloadducts. Several ethyl 2-alkyl-but-2,3-dienoates including β' -alkyl-, β' -aryl, β' -vinyl, and β' -styryl-substituted allenates were applicable to the [3+2] cycloaddition when PMe_3 was used as a nucleophilic catalyst. The use of chiral spirophosphines **16** for the asymmetric [3+2] cycloaddition resulted in high enantioselectivity in the reaction of *N,N'*-cyclic azomethine imine **17** with ethyl 2-methylbuta-2,3-dienoate (Scheme 24). In the case of diethyl 2-vinylidenesuccinate as a dipolarophile, a combination of [3+2], [3+3], and [3+4] cycloadducts was obtained (Scheme 25). In contrast to these cycloadditions, the reaction with 2.4 equiv of ethyl 2,3-butadienoate under specific conditions in a 4:1 mixed solvent of CH_2Cl_2 /benzene using PCy_3 provided [3+2+3] cycloadducts in high yield (Scheme 26).

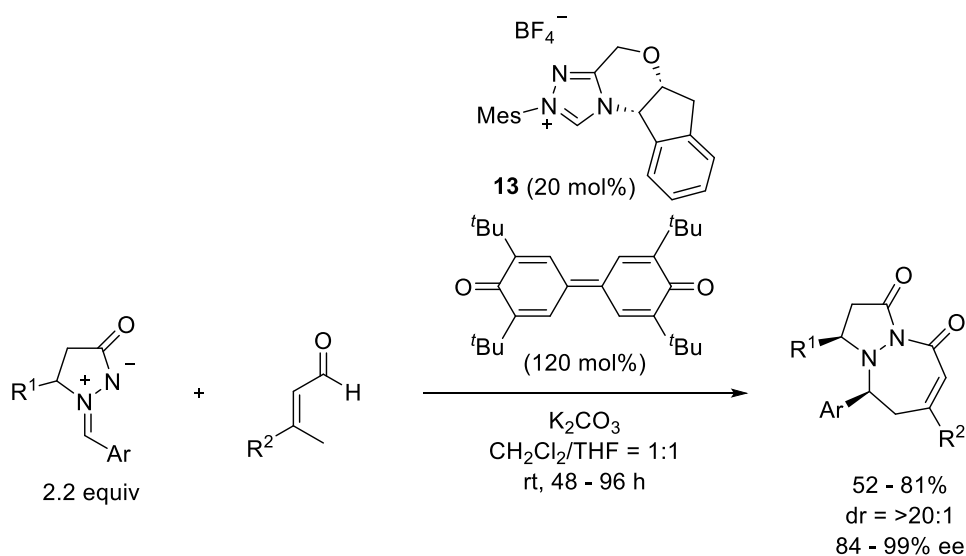


Scheme 26. Phosphine-catalyzed [3+2+3] cycloaddition with ethyl 2,3-butadienoate



Scheme 27. *N*-Heterocyclic carbene-catalyzed formal [3+3] cycloaddition with enals

In 2007, *N*-heterocyclic carbenes were reported by Chan and Scheidt to catalyze a formal [3+3] cycloaddition of *N,N'*-cyclic azomethine imines with enals, which generated a homoenolate species *in situ* by the reaction of a catalytic amount of the *N*-heterocyclic carbene generated from benzimidazolium salt **18** (Scheme 27).²⁹ The cycloaddition proceeded with high diastereoselectivity to afford bicyclic heterocycles containing a pyridazinone ring. The high levels of *syn*-selectivity for the products were explained by invoking a hydrogen-bonding assembly between the imine and the carbene-aldehyde adduct.



Scheme 28. *N*-Heterocyclic carbene-catalyzed asymmetric [3+4] cycloaddition with enals

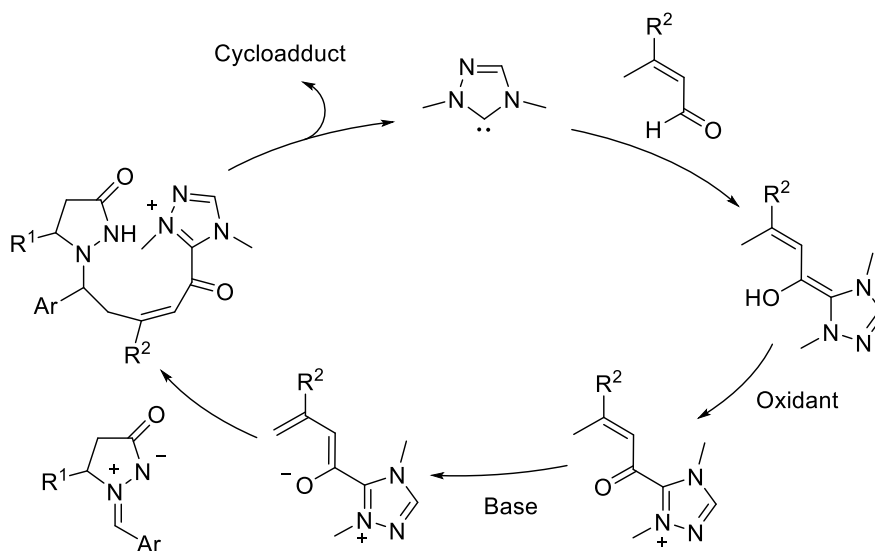
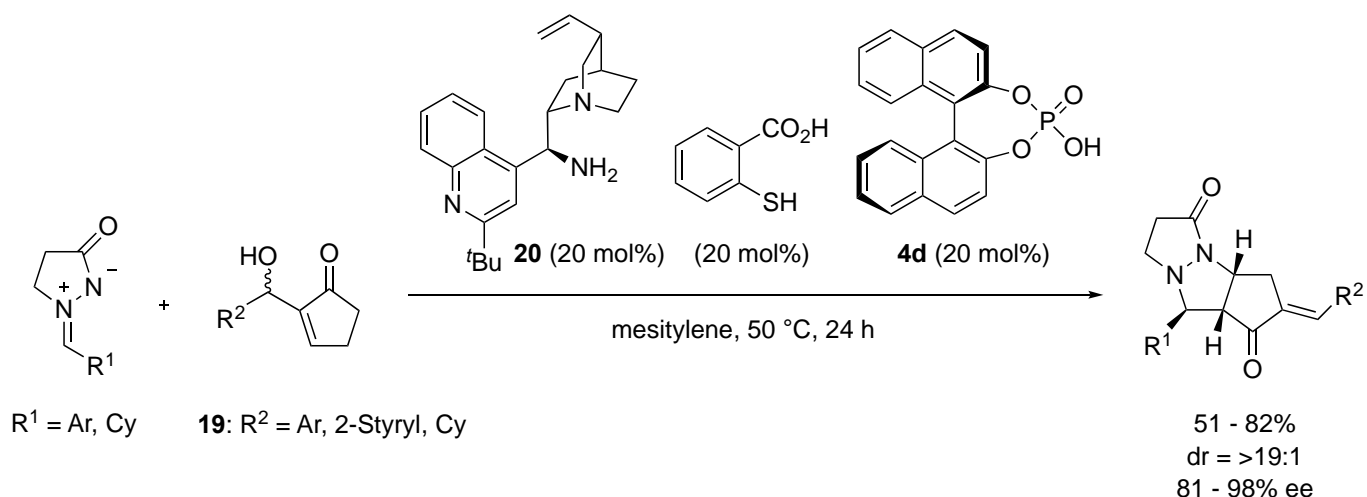


Figure 12. Postulated reaction pathway

N-Heterocyclic carbene-catalyzed asymmetric [3+4] cycloaddition of *N,N'*-cyclic azomethine imines with enals was also developed by Chi and co-workers (Scheme 28).³⁰ Oxidative catalytic remote activation of

enals by a chiral *N*-heterocyclic carbene using a quinone derivative as an oxidant afforded 1,4-dipolarophile intermediates that reacted with the azomethine imines to generate dinitrogen-fused seven-membered heterocyclic products with high optical purities. Effective kinetic resolution of the azomethine imines could be accomplished with this reaction. A postulated reaction pathway is illustrated in Figure 12.



Scheme 29. Asymmetric formal [5+3] cycloaddition with unmodified Morita-Baylis-Hillman alcohols

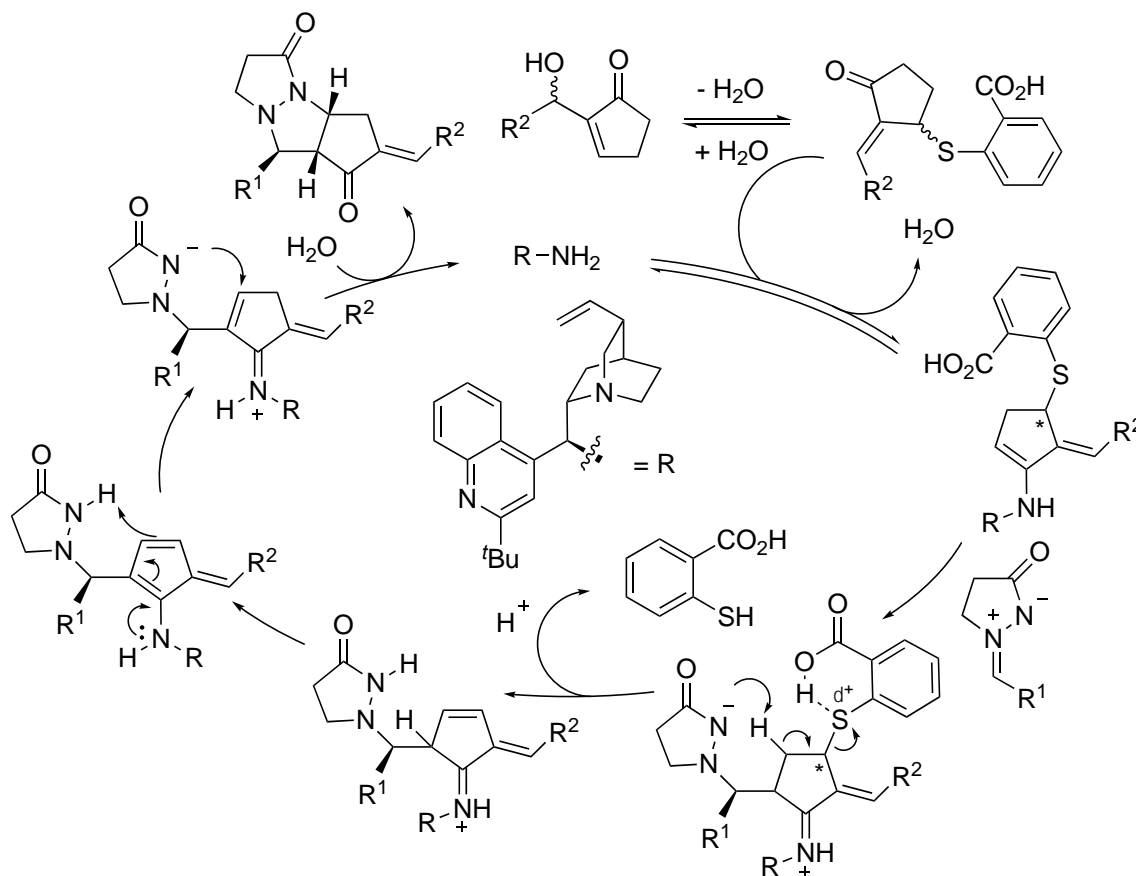
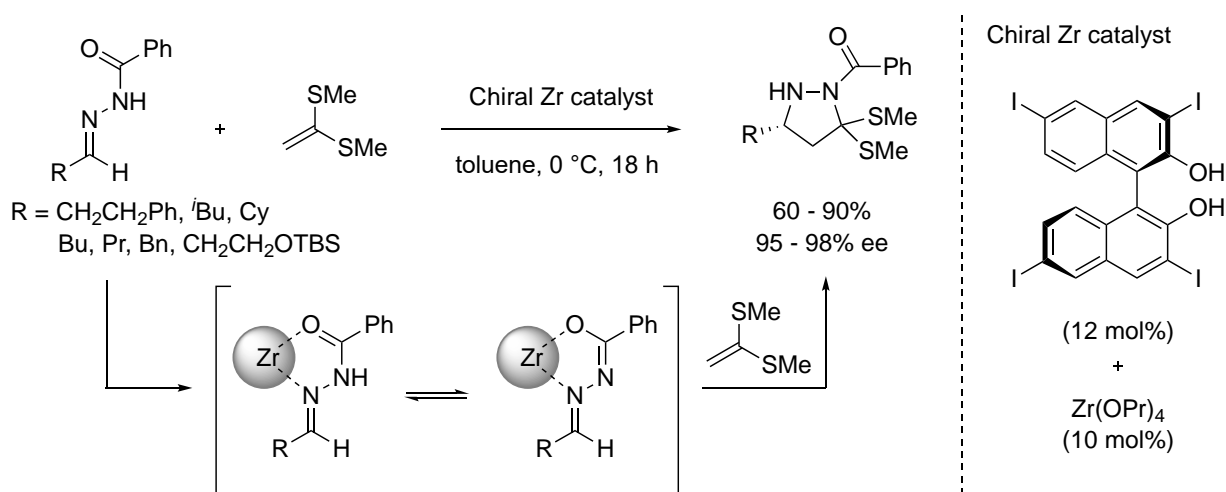


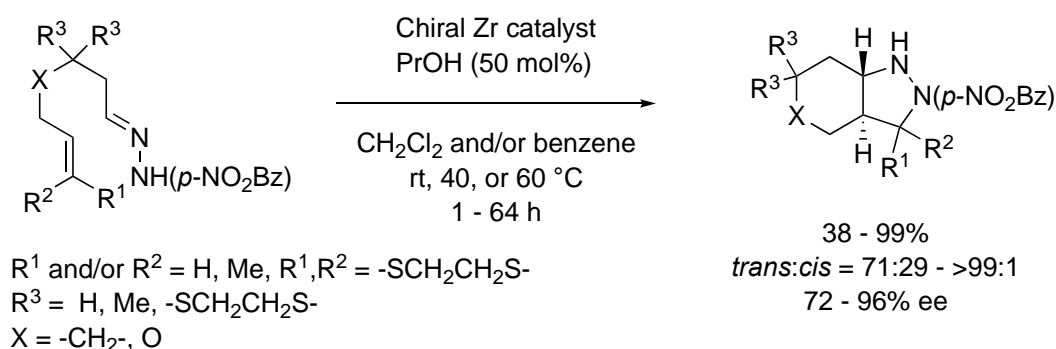
Figure 13. Proposed catalytic cycle for formal [5+3] cycloaddition

In 2019, Du, Chen, and co-workers disclosed an asymmetric formal [5+3] cycloaddition reaction of unmodified Morita-Baylis-Hillman alcohols **19** derived from 2-cyclopentenone and aldehydes with *N,N'*-cyclic azomethine imines (Scheme 29).³¹ The dual catalytic system, combining chiral primary amine **20** and achiral 2-mercaptobenzoic acid, was proven to be crucial for the chemoselectivity and enantioselectivity. Substantially substituted compounds with tricyclic frameworks were obtained with high diastereo- and enantioselectivity. A plausible catalytic cycle for the formal [5+3] cycloaddition by double activation catalysis is illustrated in Figure 13, in which the key proposed intermediates were successfully detected by high-resolution mass spectrometric analysis of the reaction mixture.

3-3. HYDRAZONES AS PRECURSORS



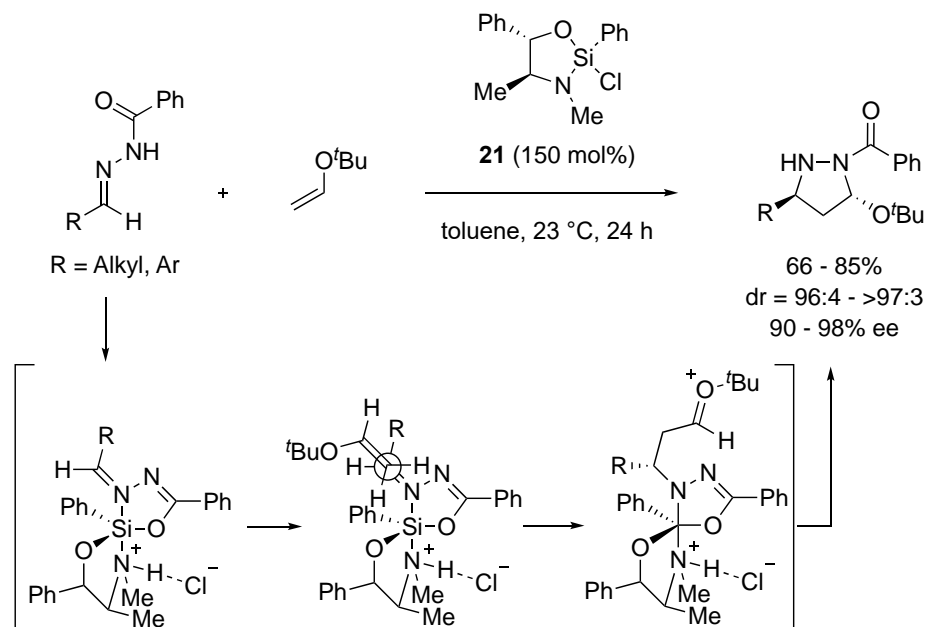
Scheme 30. Asymmetric intermolecular [3+2] cycloaddition using chiral Zr catalyst



Scheme 31. Asymmetric intramolecular [3+2] cycloaddition using chiral Zr catalyst

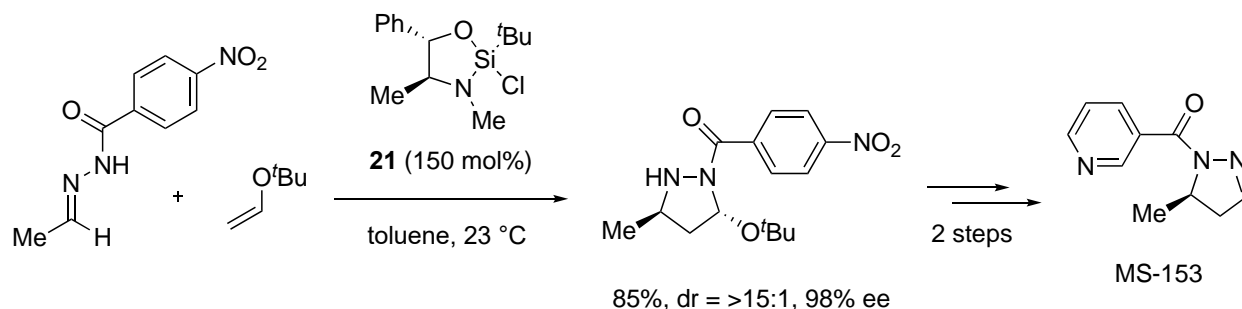
Lewis acid- and Brønsted acid-catalyzed reactions between hydrazones and alkenes were found to lead to [3+2] cycloaddition, which provided atom- and step-economical access to pyrazolidines. Kobayashi and co-workers reported that chiral zirconium/binaphthol complexes were efficient chiral Lewis acid catalysts

for both inter- and intramolecular [3+2] cycloadditions between hydrazones and alkenes to afford optically active pyrazolidines in high yields with high enantioselectivities (Schemes 30 and 31).³² The cycloadditions were proposed to proceed via concerted pathways.

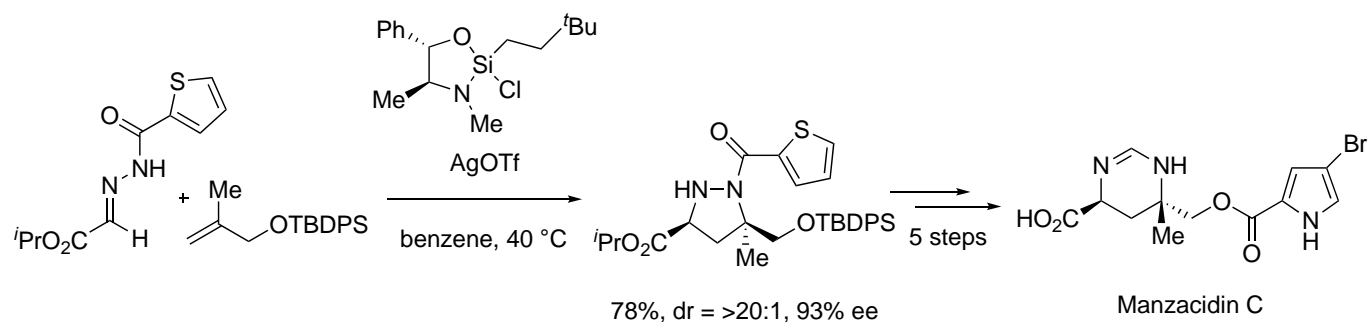


Scheme 32. Enantioselective [3+2] acylhydrazone-enol ether cycloaddition

In 2005, Leighton and co-workers reported highly enantioselective [3+2] acylhydrazone-enol ether cycloadditions using chiral silicon-based Lewis acid **21**, which was easily prepared as a 2:1 mixture of diastereomers in a single step from pseudoephedrine and phenyltrichlorosilane (Scheme 32).³³ Based on the X-ray structure obtained from the reaction of the chiral Lewis acid with the benzaldehyde-derived benzoylhydrazone, a plausible model was proposed to explain the stereoselectivity, wherein the enol ether approaches from the exposed *Si* face of the hydrazone and is oriented so as to minimize steric interactions between the bulky *t*-butoxy group and the complexed hydrazone. This protocol was applied to the synthesis of a potent neuroprotective agent MS-153 (Scheme 33)³⁴ and a bromopyrrole alkaloid manzacidin C (Scheme 34).³⁵

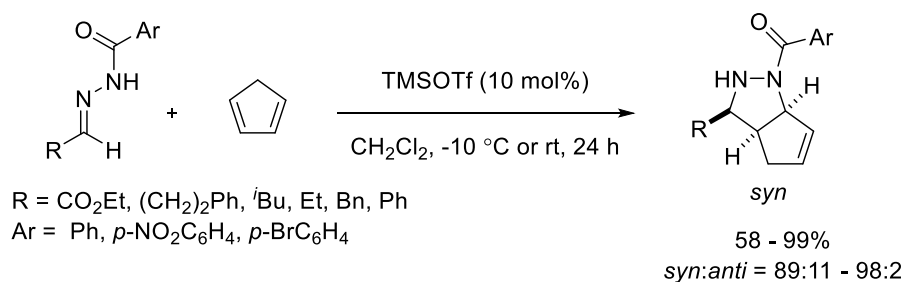


Scheme 33. Enantioselective synthesis of MS-153

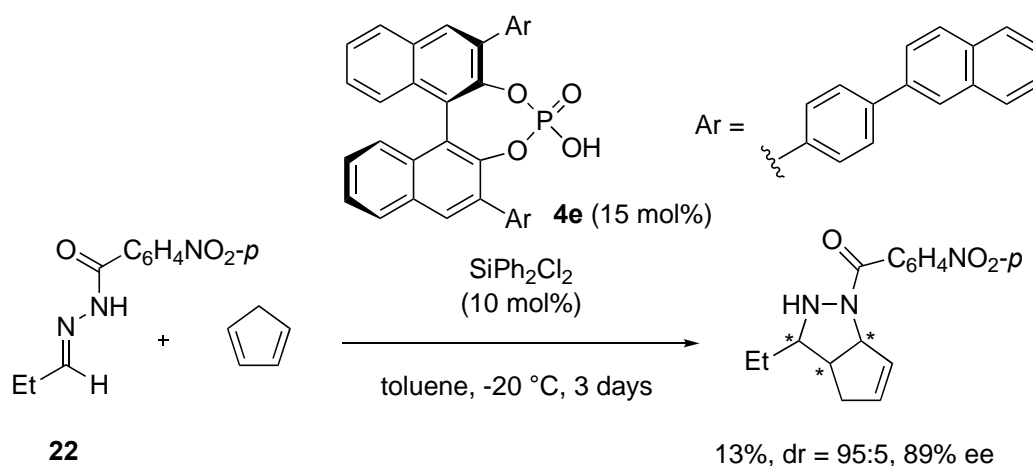


Scheme 34. Enantioselective synthesis of manzacidin C

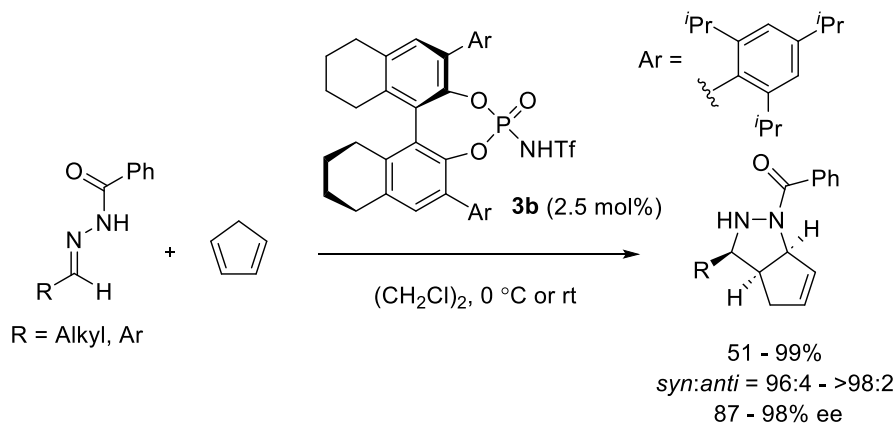
In 2011, Tsogoeva and co-workers reported the first catalytic metal-free intermolecular [3+2] cycloaddition of *N*-acylhydrazones with cyclopentadiene using TMSOTf as a catalyst in which pyrazolidine derivatives were afforded in high yields with high diastereoselectivities (Scheme 35).³⁶ In the same year, a chiral catalytic system (10 mol%), consisting of binaphthol-derived phosphoric acid **4e** and SiCl₂Ph₂, was reported to provide 89% ee with 95:5 dr of a cycloadduct in the reaction between propanal-derived benzoylhydrazone **22** and cyclopentadiene, albeit in only 13% yield (Scheme 36).³⁷



Scheme 35. Catalytic metal-free intermolecular [3+2] cycloaddition with cyclopentadiene

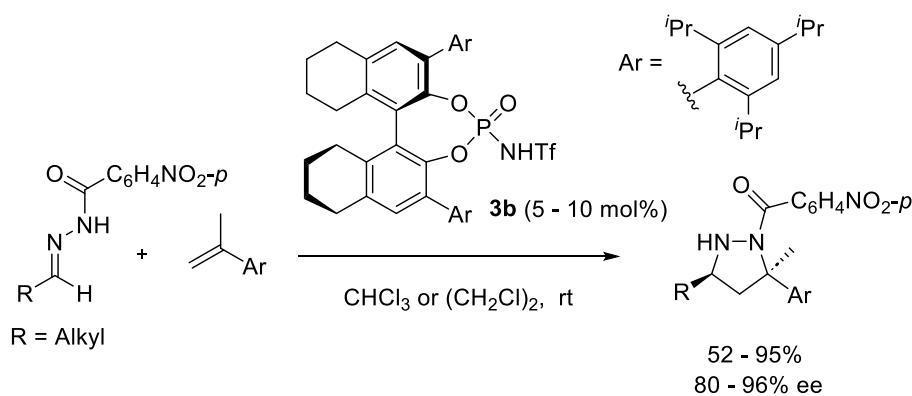


Scheme 36. Asymmetric [3+2] cycloaddition with cyclopentadiene using silicon-based Lewis acid



Scheme 37. Chiral Brønsted acid-catalyzed asymmetric [3+2] cycloaddition with cyclopentadiene

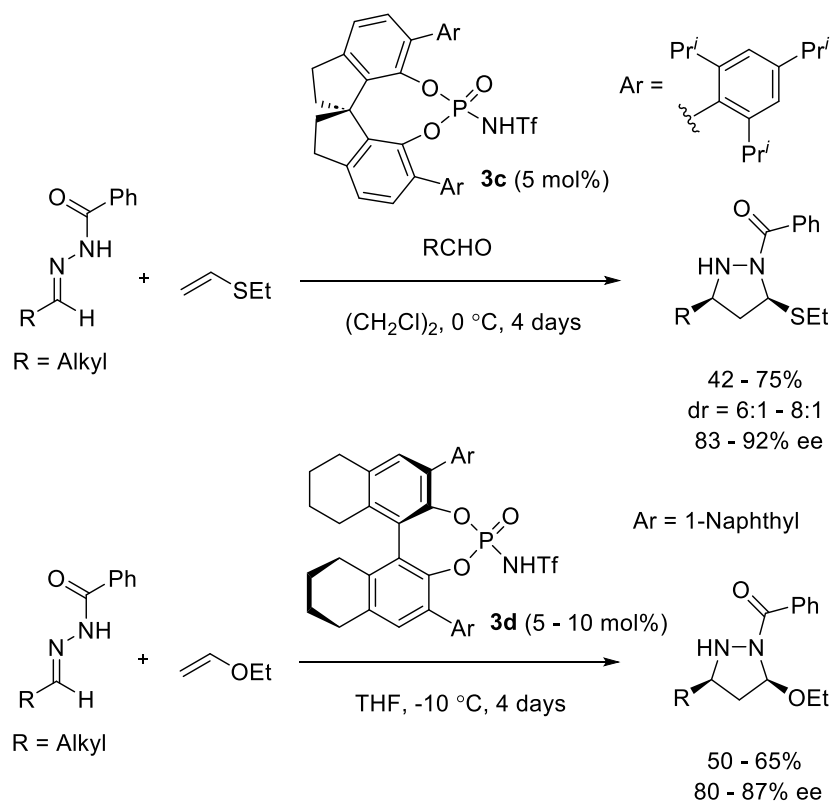
A highly enantioselective cycloaddition between *N*-benzoylhydrazones and various alkenes catalyzed by chiral *N*-triflylphosphoramidate **3b** was uncovered by Rueping and co-workers in 2012 (Schemes 37 and 38).³⁸ In contrast to phosphoric acids described by Tsogoeva in Scheme 36, the much more Brønsted acidic *N*-triflylphosphoramidates were proven to be very effective in promoting the highly enantioselective cycloaddition. Not only cyclopentadiene but also α -methylstyrene and its analogues were found to be suitable dipolarophiles for the highly diastereo- and enantioselective cycloaddition.



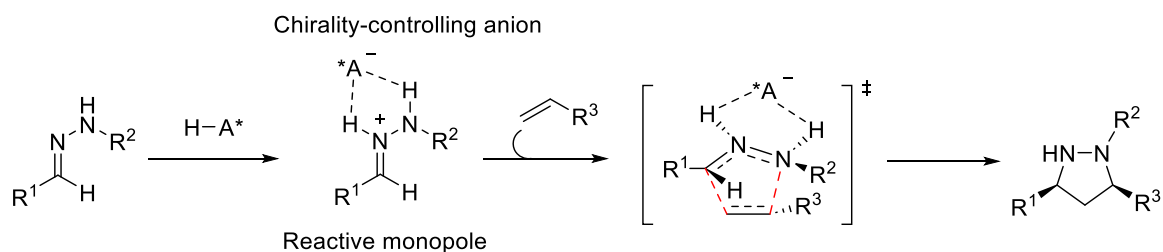
Scheme 38. Chiral Brønsted acid-catalyzed asymmetric [3+2] cycloaddition with α -methylstyrene and analogues

Rueping, Houk, and co-workers also developed a chiral Brønsted acid-catalyzed highly asymmetric [3+2] cycloaddition reaction of hydrazones with ethyl vinyl thioether and ethyl vinyl ether (Scheme 39).³⁹ The reaction can be performed with a broad range of aliphatic aldehyde-derived hydrazones using *N*-triflylphosphoramidates **3c** or **3d** to give valuable pyrazolidine derivatives in good yields with high diastereoselectivities and excellent enantioselectivities. The mechanism for achieving high catalytic efficiency and the origin of selectivity in these reactions were explored with DFT calculations (Scheme 40).

It was found that protonation of hydrazones by *N*-triflylphosphoramides produces hydrazoneium-phosphoramidate anion complexes, which are very reactive in [3+2] cycloadditions with alkenes, producing pyrazolidine products. Alternative 1,3-dipolar [3+2] cycloadditions with the analogous azomethine imines are much less favorable due to the endergonic isomerization of hydrazone to azomethine imine, while with the *N*-triflylphosphoramidate catalyst, only a small distortion of the ion-pair complex is required to achieve its geometry in the [3+2] cycloaddition transition state.



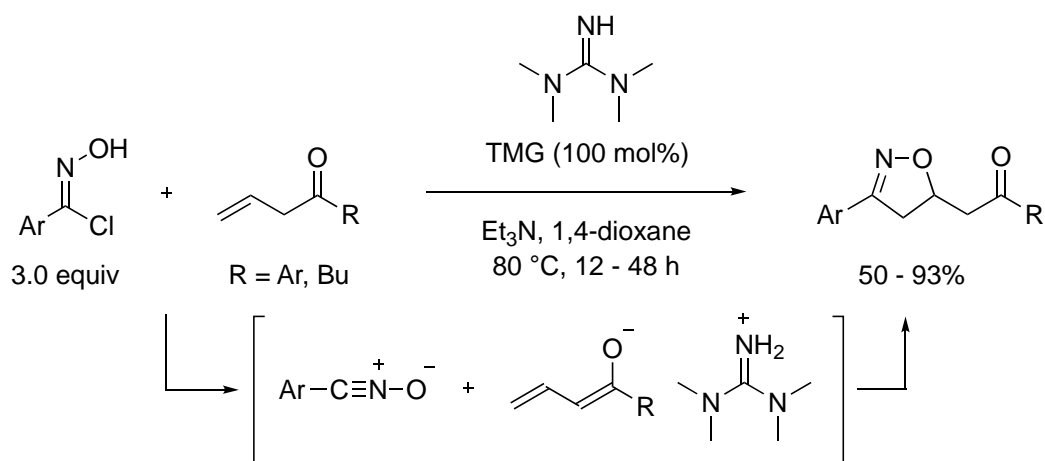
Scheme 39. Chiral Brønsted acid-catalyzed asymmetric [3+2] cycloaddition with ethyl vinyl thioether and ethyl vinyl ether



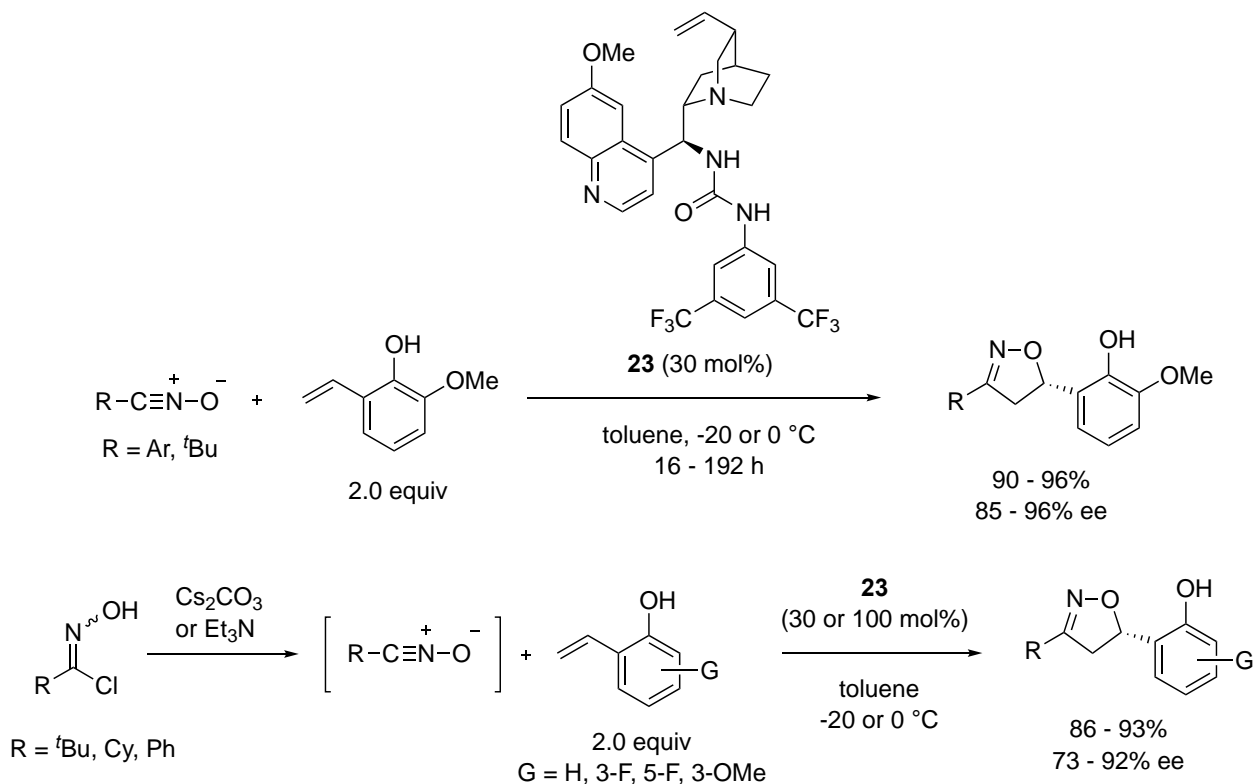
Scheme 40. Brønsted acid-catalyzed 1,3-monopolar [3+2] cycloaddition pathway

4. NITRILE OXIDE CYCLOADDITIONS

Limited examples of nitrile oxide cycloadditions using an organocatalyst have been reported to date. In 2016, Li and co-workers reported enolate-mediated 1,3-dipolar cycloaddition reactions of allyl ketones with *in situ*-generated nitrile oxides using 100 mol% 1,1,3,3-tetramethylguanidine (TMG) (Scheme 41).⁴⁰ A plausible mechanism was proposed to explain the reaction process through the generation of the enolates from allyl ketones by TMG followed by a stepwise addition of the nitrile oxides. The cycloaddition proceeded to give rapid access to 3,5-disubstituted isoxazolines in high yields with high regioselectivities.



Scheme 41. Enolate-mediated 1,3-dipolar cycloaddition of allyl ketones using TMG



Scheme 42. Asymmetric 1,3-dipolar cycloaddition with *o*-hydroxystyrenes mediated by chiral amine-urea

In 2017, the first example of asymmetric 1,3-dipolar cycloadditions between nitrile oxides and *o*-hydroxystyrenes mediated by cinchona-alkaloid-based amine-urea **23** was reported by Suga and co-workers (Scheme 42).⁴¹ The catalysis was also applicable to the reactions using unstable nitrile oxides which were generated from hydroximoyl chlorides with a base, providing the cycloadducts in high yields with good to high enantioselectivity. The authors proposed a novel dual activation strategy involving LUMO activation by a Brønsted acid and HOMO activation by a Brønsted base in the IED 1,3-dipolar cycloaddition by employing chiral amine-urea **23**. Computational studies strongly supported the HOMO activation of *o*-hydroxystyrenes and LUMO activation of nitrile oxides by hydrogen-bonding interactions with the Brønsted acid/base bifunctional catalyst (Figure 14). The $\Delta\Delta G^\ddagger$ energy for the *anti*-open TS (*S*) conformation was favored over other TS (*R*) conformations. The improved procedure for *in situ*-generated nitrile oxides revealed that the dual activation strategy is more suitable for nitrile oxides bearing aliphatic substituents, probably due to the lower reactivity that prevented the background reaction (Scheme 43).⁴²

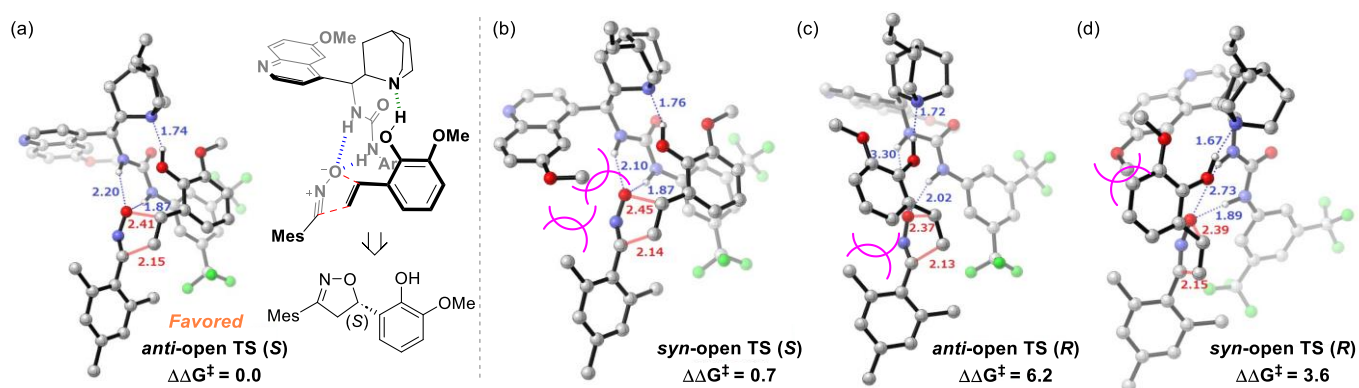
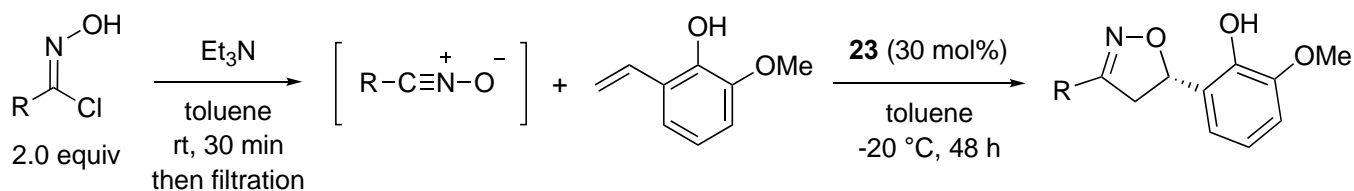


Figure 14. Transition states corresponding to *anti*-open and *syn*-open conformers by DFT calculations (All energies are shown in kcal mol⁻¹. Bond lengths are shown in Å.)



R = Cy, Pentyl, ^tBu, Bn: 49 - 89%, 73 - 90% ee

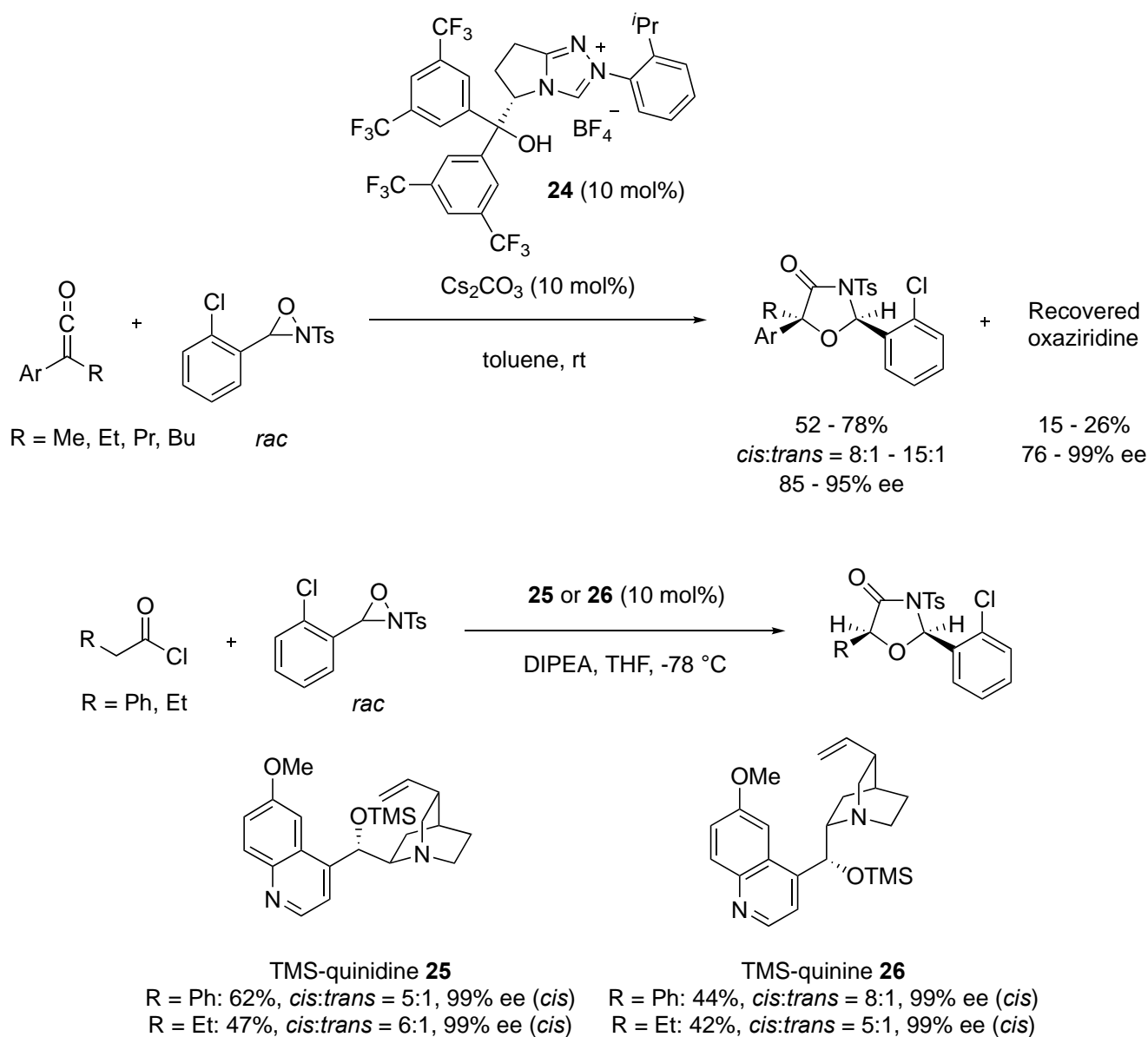
R = Ph, 4-Tolyl, 3-Tolyl, 2-Tolyl, (*E*)-Cinnamyl: 81 - 98%, 48 - 57% ee

Scheme 43. Chiral amine-urea-catalyzed asymmetric cycloaddition of *in situ*-generated nitrile oxides

5. SIMILAR TYPES OF FORMAL [3+2] CYCLOADDITIONS

5-1. OXAZIRIDINES AS 1,3-DIPOLE EQUIVALENTS

Formal [3+2] cycloadditions of ketenes and oxaziridines catalyzed by chiral Lewis bases, which achieved the enantioselective synthesis of oxazolidin-4-ones, were reported by Ye and co-workers in 2010 (Scheme 44).⁴³ The chiral *N*-heterocyclic carbene generated from triazolium salt **24** and cinchona alkaloids **25** or **26** were found to be effective Lewis base catalysts for the reactions of stable disubstituted ketenes and unstable monosubstituted ketenes, respectively. Both enantiomers of oxazolidin-4-ones could be obtained in moderate to good yields with good diastereo- and enantioselectivities by choosing the appropriate catalysts. The proposed catalytic cycle is shown in Figure 15.



Scheme 44. Formal [3+2] cycloaddition reaction of ketenes and oxaziridines catalyzed by chiral Lewis bases

In 2013, Lui, Feng, and co-workers reported an asymmetric oxyamination of azlactones with oxaziridines using chiral bisguanidinium salt **5c** as an organocatalyst. The reaction proceeded through a formal [3+2] cycloaddition that allowed the generation of a variety of optically active oxazolin-4-one derivatives (Scheme 45).⁴⁴ The reaction also displayed remarkable triple stereo-differentiation and kinetic resolution to afford a series of oxaziridines with optical purities of up to 99% ee.

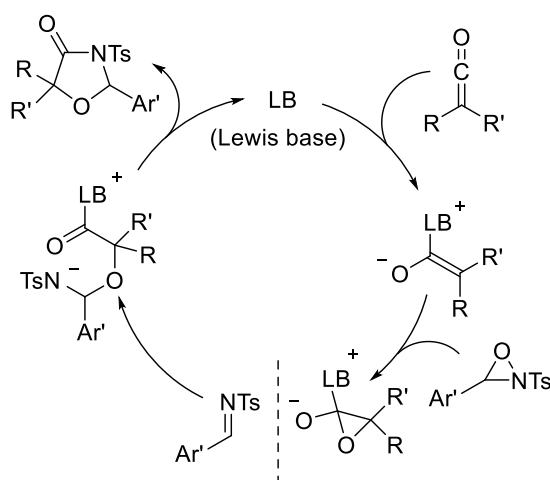
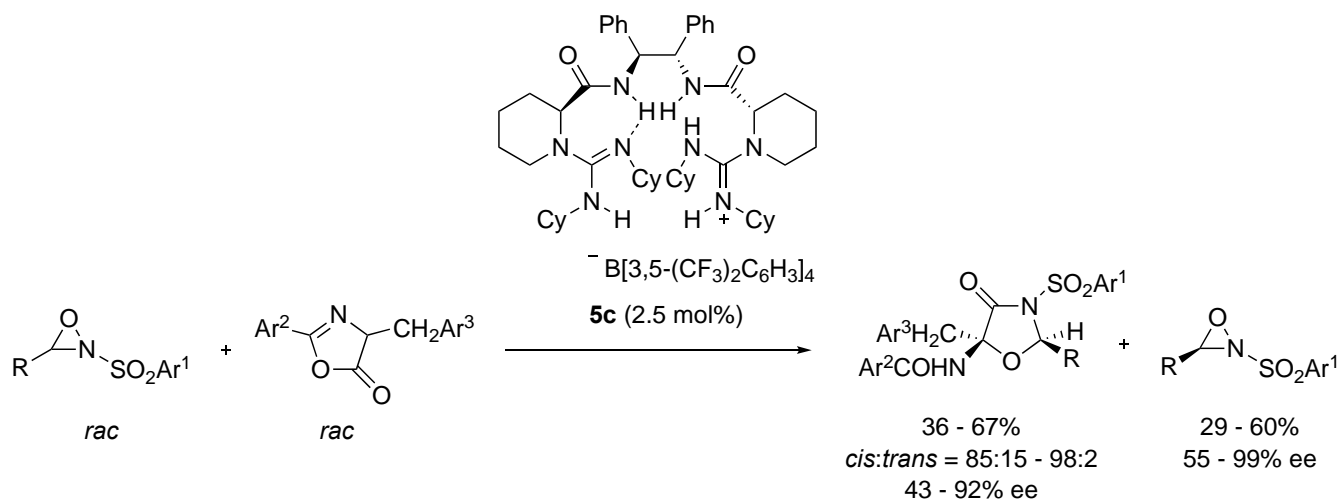


Figure 15. Possible catalytic cycle for formal [3+2] cycloaddition reaction

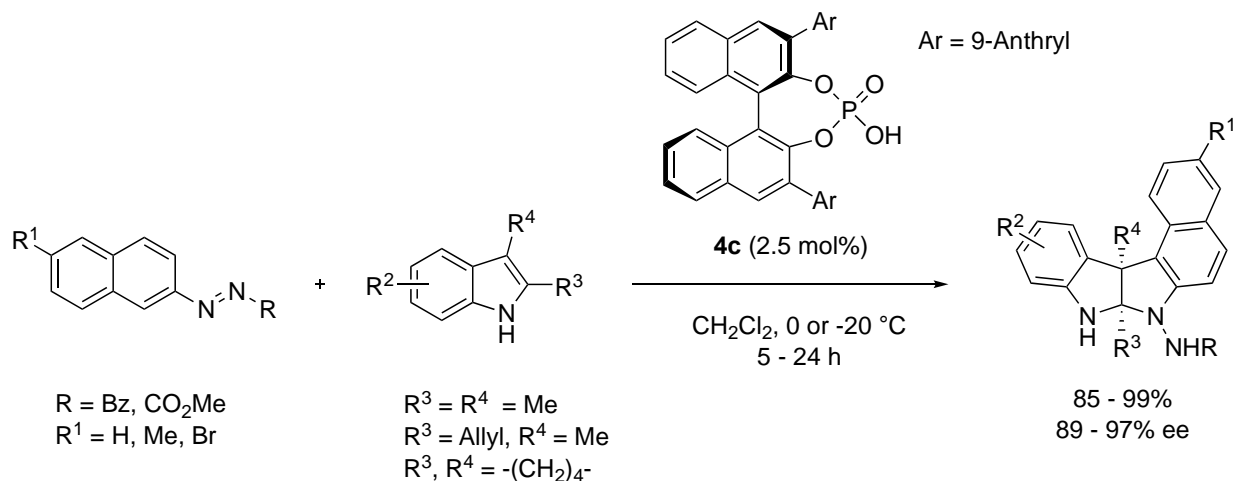


Scheme 45. Asymmetric oxyamination of azlactones with oxaziridines

5-2. AZO COMPOUNDS AS 1,3-DIPOLE EQUIVALENTS

It is known that azobenzenes and azonaphthalenes can act as 1,3-dipole surrogates in [3+2] cyclizations with olefins. In 2018, Tan and co-workers reported an enantioselective [3+2] cyclization of azonaphthalenes with 2,3-disubstituted indoles by chiral phosphoric acid catalyst **4c** (Scheme 46).⁴⁵ The organocatalytic annulation reaction, triggered by formal nucleophilic aromatic substitution of azonaphthalene derivatives with 2,3-disubstituted indoles, delivered enantioenriched pyrroloindoles

bearing two contiguous quaternary chiral centers with high enantioselectivity. A plausible reaction mechanism was proposed, as illustrated in Figure 16.



Scheme 46. Enantioselective [3+2] cyclization of azonaphthalenes with 2,3-disubstituted indoles

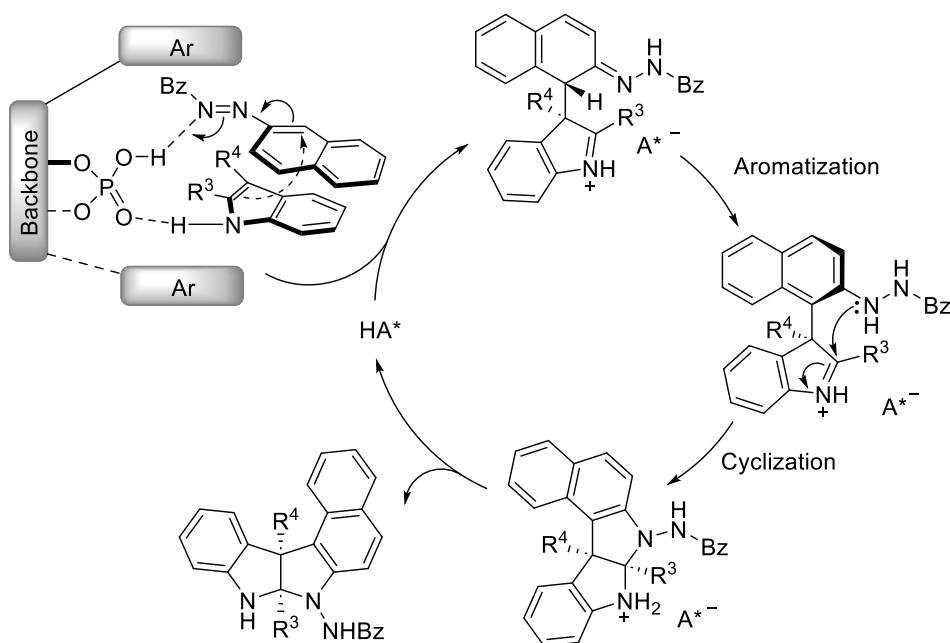
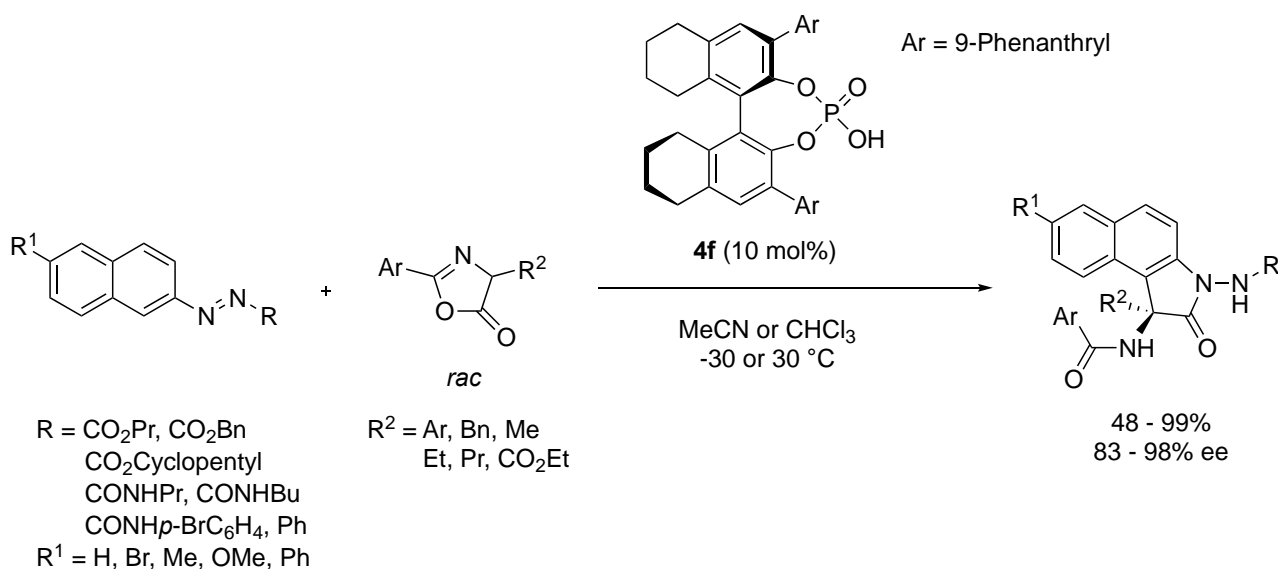


Figure 16. Plausible reaction mechanism for enantioselective [3+2] cyclization

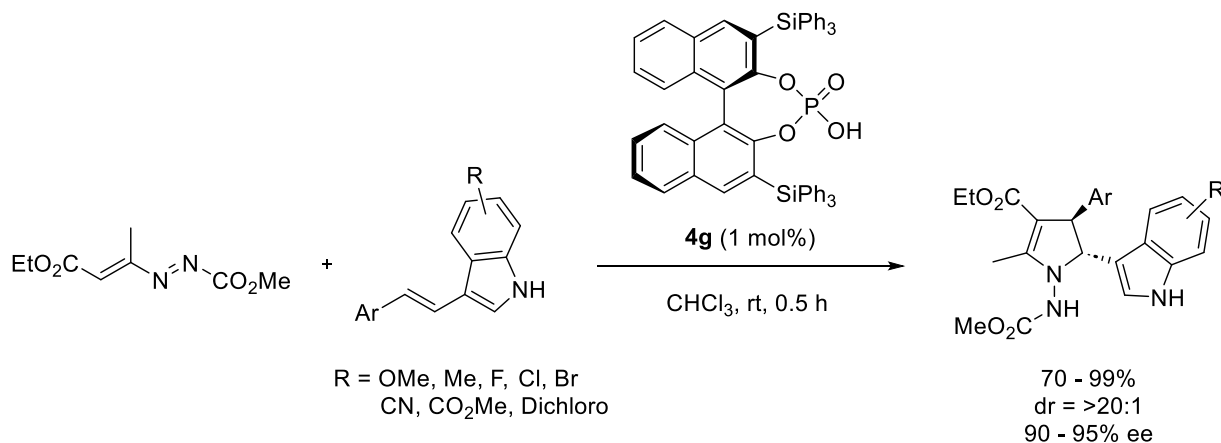
The first catalytic asymmetric [2+3] cyclization using azlactones as C2 building blocks and azonaphthalenes as 1,3-dipole surrogates by chiral phosphoric acid **4f** was reported by Mei, Shi, and co-workers in 2018 (Scheme 47).⁴⁶ This strategy allowed the synthesis of a variety of chiral isatin derivatives in generally good yields and excellent enantioselectivities (up to 99% yield, 98% ee).

A chiral phosphoric acid-catalyzed highly enantioselective formal [3+2] cycloaddition reaction of azoalkenes with 3-vinylindoles was also uncovered by Lu and co-workers in 2020 (Scheme 48).⁴⁷ The

reaction using chiral phosphoric acid catalyst **4g** proceeded in a highly enantioselective and diastereospecific manner, providing a wide range of functionalized 2,3-dihydropyrroles in good yields. The methodology could be identified as a formal IED 1,3-dipolar cycloaddition reaction, wherein azoalkenes serve as 1,3-dipole surrogates of CCN 3-atom synthons in contrast to the common 4-atom synthons in previous literature reports.



Scheme 47. Asymmetric [2+3] cyclization of azlactones with azonaphthalenes



Scheme 48. Enantioselective formal [3+2] cycloaddition reaction of azoalkenes with 3-vinylindoles

6. CONCLUSION

In this review, we described asymmetric IED 1,3-dipolar cycloadditions using organocatalysts. Reported examples of the cycloadditions of nitrones were limited in both organocatalysis and Lewis acid catalysis. For the organocatalytic asymmetric IED cycloadditions of nitrones, vinyl ethers and azlactones were employed as dipolarophiles with the use of binaphthol-derived chiral Brønsted acids and chiral amide-

guanidines. For organocatalysis, the enantioselective cycloadditions between *C,N*-diarylnitrones and ethyl vinyl ether in the presence of a chiral *N*-triflylphosphoramidate reported by Yamamoto and co-workers in 2008 is a seminal work. More examples of organocatalysis were reported for azomethine imines compared with other 1,3-dipoles among the asymmetric IED cycloadditions. Encarbamates, enamines and dienamines generated by chiral amine catalysts, chiral enols (or enolates) generated by *N*-heterocyclic carbenes, and enol forms (or enolate forms) of azlactones could be used as dipolarophiles, since Maruoka, Hashimoto, and co-workers reported the asymmetric cycloadditions of tetrahydroisoquinoline-based *C,N*-cyclic azomethine imines with electron-rich alkenes such as *t*-butyl vinyl ether and vinylogous aza-enamines. The asymmetric cycloadditions of *N,N'*-cyclic azomethine imines were reported involving the reaction with allenates in combination with chiral phosphine, the reaction with 2-hydroxystyrene in the presence of chiral phosphoric acid, and the reaction using hydrazones as azomethine imine precursors. Only one example of organocatalyst-mediated IED cycloaddition of nitrile oxides was reported in the reactions with 2-hydroxystyrenes under the influence of quinine-derived chiral amine-ureas based on a bifunctional activation strategy. For IED-type reactions by organocatalysis, oxaziridines and azo compounds could be utilized as 1,3-dipole equivalents in enantioselective formal [3+2] cycloaddition reactions. Depending on the 1,3-dipoles, the enantioselective IED cycloadditions using organocatalysts are still underdeveloped. We hope that this field of chemistry will be developed significantly in the future.

ACKNOWLEDGEMENTS

This work was supported in part by the Japan Society for the Promotion of Science (JSPS) through Grants-in-Aid for Scientific Research (C) (Grant Nos. JP19K05454, JP21K05067, and JP22K05090).

REFERENCES

1. (a) R. Huisgen, H.-J. Hansen, H. Heimgartner, P. Caramella, P. Grünanger, M. Regitz, H. Heydt, W. Lwowski, J. W. Lown, and R. Grashey, '1,3-Dipolar Cycloaddition Chemistry,' Vol 1, ed. by A. Padwa, Wiley, Inc., New York, 1984, p. 1; (b) K. T. Potts, J. J. Tufariello, R. C. Storr, R. L. Kuczkowski, A. Padwa, K. N. Houk, K. Yamaguchi, G. Bianchi, R. Gandolfi, and J. N. Crabb, '1,3-Dipolar Cycloaddition Chemistry,' Vol 2, ed. by A. Padwa, Wiley, Inc., New York, 1984, pp. 1.
2. J. N. Martin, R. C. F. Jones, S. E. Denmark, J. J. Cottell, L. M. Harwood, R. J. Vickers, M. C. McMills, D. Wright, G. Mloston, H. Heimgartner, V. Jäger, P. A. Colinas, J. T. Sharp, G. Maas, C.-K. Sha, A. K. Mohanakrishnan, G. W. Gribble, S. Kanemasa, K. V. Gothelf, and K. A. Jørgensen, 'Synthetic Application of 1,3-Dipolar Cycloaddition Chemistry Toward Heterocycles and Natural Products,' ed. by A. Padwa and W. H. Pearson, Wiley, Inc., Hoboken, 2003, p. 1.
3. (a) K. V. Gothelf and K. A. Jørgensen, *Chem. Rev.*, 1998, **98**, 863; (b) H. Pellissier, *Tetrahedron*, 2007,

- 63, 3235; (c) M. Kissane and A. R. Maguire, *Chem. Soc. Rev.*, 2010, **39**, 845.
4. (a) L. M. Stanley and M. P. Sibi, *Chem. Rev.*, 2008, **108**, 2887; (b) C. Nájera, J. M. Sansano, and M. Yus, *J. Braz. Chem. Soc.*, 2010, **21**, 377; (c) T. Hashimoto and K. Maruoka, *Chem. Rev.*, 2015, **115**, 5366.
 5. (a) R. Sustmann, *Tetrahedron Lett.*, 1971, 2717; (b) K. N. Houk, J. Sims, R. E. Duke Jr., R. W. Strozier, and J. K. George, *J. Am. Chem. Soc.*, 1973, **95**, 7287; (c) K. N. Houk, J. Sims, C. R. Watts, and L. J. Luskus, *J. Am. Chem. Soc.*, 1973, **95**, 7301; (d) R. Sustmann, *Pure Appl. Chem.*, 1974, **40**, 569.
 6. I. Fleming, 'Frontier Orbitals and Organic Chemical Reactions,' Wiley, Inc., Chichester, 1976, p. 1; I. Fleming, 'Molecular Orbitals and Organic Chemical Reactions, Student Edition' Wiley, Inc., Chichester, 2009, p. 1.
 7. (a) J.-P. G. Seerden, A. W. A. Scholte op Reimer, and H. W. Scheeren, *Tetrahedron Lett.*, 1994, **35**, 4419; (b) J.-P. G. Seerden, M. M. M. Kuypers, and H. W. Scheeren, *Tetrahedron: Asymmetry*, 1995, **6**, 1441; (c) J.-P. G. Seerden, M. M. M. Boeren, and H. W. Scheeren, *Tetrahedron*, 1997, **53**, 11843.
 8. (a) K. B. Simonsen, P. Bayón, R. G. Hazell, K. V. Gothelf, and K. A. Jørgensen, *J. Am. Chem. Soc.*, 1999, **121**, 3845; (b) K. B. Jensen, M. Roberson, and K. A. Jørgensen, *J. Org. Chem.*, 2000, **65**, 9080.
 9. K. B. Jensen, R. G. Hazell, and K. A. Jørgensen, *J. Org. Chem.*, 1999, **64**, 2353.
 10. P. Jiao, D. Nakashima, and H. Yamamoto, *Angew. Chem. Int. Ed.*, 2008, **47**, 2411.
 11. Y. Jin, Y. Honma, H. Morita, M. Miyagawa, and T. Akiyama, *Synlett*, 2019, **30**, 1541.
 12. H.-W. Zhao, Y.-Y. Liu, Y.-D. Zhao, H.-L. Pang, X.-Q. Chen, X.-Q. Song, T. Tian, B. Li, Z. Yang, J. Du, and N.-N. Feng, *Org. Lett.*, 2017, **19**, 26.
 13. L. Xie, Y. Li, S. Dong, X. Feng, and X. Liu, *Chem. Commun.*, 2021, **57**, 239.
 14. S. Postikova, T. Tite, V. Levacher, and J.-F. Brière, *Adv. Synth. Catal.*, 2013, **355**, 2513.
 15. T. Hashimoto, M. Omote, and K. Maruoka, *Angew. Chem. Int. Ed.*, 2011, **50**, 3489.
 16. Y. Wang, Q. Wang, and J. Zhu, *Chem. Eur. J.*, 2016, **22**, 8084.
 17. W. Li, Q. Jia, Z. Du, K. Zhang, and J. Wang, *Chem. Eur. J.*, 2014, **20**, 4559.
 18. W. Li, J. Wei, Q. Jia, Z. Du, K. Zhang, and J. Wang, *Chem. Eur. J.*, 2014, **20**, 6592.
 19. C. Izquierdo, F. Esteban, A. Parra, R. Alfaro, J. Alemán, A. Fraile, and J. L. G. Ruano, *J. Org. Chem.*, 2014, **79**, 10417.
 20. G. Feng, G. Ma, W. Chen, S. Xu, K. Wang, and S. Wang, *Molecules*, 2021, **26**, 2969.
 21. L. Hesping, A. Biswas, C. G. Daniliuc, C. Mück-Lichtenfeld, and A. Studer, *Chem. Sci.*, 2015, **6**, 1252.
 22. B.-S. Li, Y. Wang, Z. Jina, and Y. R. Chi, *Chem. Sci.*, 2015, **6**, 6008.
 23. Z.-H. Gao, X.-Y. Chen, J.-T. Cheng, W.-L. Liao, and S. Ye, *Chem. Commun.*, 2015, **51**, 9328.
 24. D. Wang, Y. Lei, Y. Wei, and M. Shi, *Chem. Eur. J.*, 2014, **20**, 15325.
 25. X. Liu, Y. Wang, D. Yang, J. Zhang, D. Liu, and W. Su, *Angew. Chem. Int. Ed.*, 2016, **55**, 8100.

26. R.-Y. Zhu, C.-S. Wang, J. Zheng, F. Shi, and S.-J. Tu, *J. Org. Chem.*, 2014, **79**, 9305.
 27. Q. Zhang, S. Guo, J. Yang, K. Yu, X. Feng, L. Lin, and X. Liu, *Org. Lett.*, 2017, **19**, 5826.
 28. R. Na, C. Jing, Q. Xu, H. Jiang, X. Wu, J. Shi, J. Zhong, M. Wang, D. Benitez, E. Tkatchouk, W. A. Goddard, III, H. Guo, and O. Kwon, *J. Am. Chem. Soc.*, 2011, **133**, 13337.
 29. A. Chan and K. A. Scheidt, *J. Am. Chem. Soc.*, 2007, **129**, 5334.
 30. M. Wang, Z. Huang, J. Xu, and Y. R. Chi, *J. Am. Chem. Soc.*, 2014, **136**, 1214.
 31. Q.-Q. Yang, X. Yin, X.-L. He, W. Du, and Y.-C. Chen, *ACS Catal.*, 2019, **9**, 1258.
 32. (a) S. Kobayashi, H. Shimizu, Y. Yamashita, H. Ishitani, and J. Kobayashi, *J. Am. Chem. Soc.*, 2002, **124**, 13678; (b) Y. Yamashita and S. Kobayashi, *J. Am. Chem. Soc.*, 2004, **126**, 11279.
 33. S. Shirakawa, P. J. Lombardi, and J. L. Leighton, *J. Am. Chem. Soc.*, 2005, **127**, 9974.
 34. K. Tran and J. L. Leighton, *Adv. Synth. Catal.*, 2006, **348**, 2431.
 35. K. Tran, P. J. Lombardi, and J. L. Leighton, *Org. Lett.*, 2008, **10**, 3156.
 36. A. Zamfir, S. Schenker, W. Bauer, T. Clark, and S. B. Tsogoeva, *Eur. J. Org. Chem.*, 2011, 3706.
 37. A. Zamfir and S. B. Tsogoeva, *Synthesis*, 2011, 1988.
 38. M. Rueping, M. S. Maji, H. B. Küçük, and I. Atodiresei, *Angew. Chem. Int. Ed.*, 2012, **51**, 12864.
 39. X. Hong, H. B. Küçük, M. S. N. Maji, Y.-F. Yang, M. Rueping, and K. N. Houk, *J. Am. Chem. Soc.*, 2014, **136**, 13769.
 40. W. Li, X. Zhou, Z. Shi, Y. Liu, Z. Liu, and H. Gao, *Org. Biomol. Chem.*, 2016, **14**, 9985.
 41. H. Suga, Y. Hashimoto, Y. Toda, K. Fukushima, H. Esaki, and A. Kikuchi, *Angew. Chem. Int. Ed.*, 2017, **56**, 11936.
 42. Y. Toda, M. Koyama, H. Esaki, K. Fukushima, and H. Suga, *Heterocycles*, 2018, **97**, 147.
 43. P.-L. Shao, X.-Y. Chen, and S. Ye, *Angew. Chem. Int. Ed.*, 2010, **49**, 8412.
 44. S. Dong, X. Liu, Y. Zhu, P. He, L. Lin, and X. Feng, *J. Am. Chem. Soc.*, 2013, **135**, 10026.
 45. L.-W. Qi, J.-H. Mao, J. Zhang, and B. Tan, *Nat. Chem.*, 2018, **10**, 58.
 46. C. Ma, J.-Y. Zhou, Y.-Z. Zhang, G.-J. Mei, and F. Shi, *Angew. Chem. Int. Ed.*, 2018, **57**, 5398.
 47. G.-J. Mei, W. Zheng, T. P. Gonçalves, X. Tang, K.-W. Huang, and Y. Lu, *Science*, 2020, **23**, 100873.
-



Professor Hiroyuki Suga was obtained his Ph. D. degree in 1988 from Kyushu University. He joined the Institute of Chemistry, College of General Education, Osaka University as an assistant professor in 1988. He also spent his research carrier as an assistant professor at the Department of Chemistry, Faculty of Science, Osaka University from 1994, and the Department of Chemistry, Graduate School of Science, Osaka University from 1996. He was promoted to an associate professor at the Department of Chemistry and Material Engineering, Faculty of Engineering, Shinshu University in 1998. From 2006, he is a professor at the same university, and currently a professor at the Department of Materials Chemistry, Faculty of Engineering, Shinshu University. His research interest is the synthesis of optically active heterocyclic compounds with biological activity.



Yasunori Toda received his B.S. Chemistry degree from Tohoku University in March 2008. He continued into graduate studies at Tohoku University, where he worked with Prof. Masahiro Terada. He joined the Johnston group at Vanderbilt University in June 2013. In April 2015, he began a position as assistant professor of chemistry at Shinshu University and is currently associate professor at the Department of Materials Chemistry, Faculty of Engineering, Shinshu University.